1985

New detection methods and techniques with applications in liquid chromatography

Steven A. Wilson
Iowa State University

INFORMATION TO USERS

This reproduction was made from a copy of a manuscript sent to us for publication and microfilming. While the most advanced technology has been used to photograph and reproduce this manuscript, the quality of the reproduction is heavily dependent upon the quality of the material submitted. Pages in any manuscript may have indistinct print. In all cases the best available copy has been filmed.

The following explanation of techniques is provided to help clarify notations which may appear on this reproduction.

1. Manuscripts may not always be complete. When it is not possible to obtain missing pages, a note appears to indicate this.

2. When copyrighted materials are removed from the manuscript, a note appears to indicate this.

3. Oversize materials (maps, drawings, and charts) are photographed by sectioning the original, beginning at the upper left hand corner and continuing from left to right in equal sections with small overlaps. Each oversize page is also filmed as one exposure and is available, for an additional charge, as a standard 35mm slide or in black and white paper format.*

4. Most photographs reproduce acceptably on positive microfilm or microfiche but lack clarity on xerographic copies made from the microfilm. For an additional charge, all photographs are available in black and white standard 35mm slide format.*

*For more information about black and white slides or enlarged paper reproductions, please contact the Dissertations Customer Services Department.

Wilson, Steven A.

NEW DETECTION METHODS AND TECHNIQUES WITH APPLICATIONS IN LIQUID CHROMATOGRAPHY

Iowa State University

PH.D. 1985

PLEASE NOTE:

In all cases this material has been filmed in the best possible way from the available copy. Problems encountered with this document have been identified here with a check mark __✓__.

1. Glossy photographs or pages _____
2. Colored illustrations, paper or print _____
3. Photographs with dark background _____
4. Illustrations are poor copy _____
5. Pages with black marks, not original copy _____
6. Print shows through as there is text on both sides of page _____
7. Indistinct, broken or small print on several pages ✓
8. Print exceeds margin requirements _____
9. Tightly bound copy with print lost in spine _____
10. Computer printout pages with indistinct print _____
11. Page(s) _____ lacking when material received, and not available from school or author.
12. Page(s) _____ seem to be missing in numbering only as text follows.
13. Two pages numbered _____. Text follows.
14. Curling and wrinkled pages _____
15. Dissertation contains pages with print at a slant, filmed as received _____
16. Other _____

_____

_____

University
Microfilms
International

New detection methods and techniques with applications in liquid chromatography

by

Steven A. Wilson

A Dissertation Submitted to the
Graduate Faculty in Partial Fulfillment of the
Requirements for the Degree of
DOCTOR OF PHILOSOPHY

Department: Chemistry
Major: Analytical Chemistry

Approved:

Signature was redacted for privacy.

In Charge of Major Work

Signature was redacted for privacy.

For the Major Department

Signature was redacted for privacy.

For the Graduate College

Iowa State University
Ames, Iowa

1985

TABLE OF CONTENTS

DEDICATION

To my younger brother, Ken, for his courage in continually overcoming the handicap of learning disabilities.

PREFACE

The science of separations has made vast improvements in the past few decades. Intense research interest has focused on making improvements in liquid chromatographic systems. This dissertation describes research which has improved the weakest component in the chromatographic system, i.e., analyte detection.

The research can be divided into two basic areas. Part I describes instrumental techniques, which allow improved measurement capabilities, and Part II discusses a novel detection method, which allows one to better utilize the measurements.

PART I. NEW LASER-BASED DETECTION TECHNIQUES

INTRODUCTION TO LASER-BASED OPTICAL DETECTORS

Since the pioneering work by M. S. Tswett in adsorption chromatography around the turn of the century (1-3), chromatography has gone through phases of intense interest and growth to neglect. Liquid chromatography (LC) is presently receiving the attention that gas chromatography (GC) received in the late 1950s and early 1960s. The reason for this interest is the realization that GC cannot meet the sample separation and detection needs for all six million compounds listed in the chemical registry. Analysis of samples with large thermally labile molecules has required the development of improved performance from LC systems. Probably the weakest component in LC systems is that of detection. GC has the flame ionization detector as a universal detector and the mass spectrometer as a selective detector, which in combination meets the needs for an ideal detector. Developing an ideal detector for LC has required more than merely transferring the GC detectors, due to the many physical differences of an analyte in a gas eluent versus in a liquid eluent.

The most important property in developing an ideal detector for LC would be good detectability. The reason why it has been more difficult to develop a detector with good detectability for LC compared to GC, is the close similarity

between the analyte and the eluent. The LC detector with the best detectability, presently, is based on fluorescence measurements. Although one can measure injected analyte masses easily in the picogram range with this detector, it can only detect the few molecules that fluoresce. An ideal detector would have this detectability for all analytes.

The next characteristic, selectivity, is more important for an LC detector than it is for a GC detector, due to the poorer resolving power of LC columns, at present, compared to GC capillary columns. This property would be used to detect the presence of an analyte eluting at the same time as interfering compounds.

With the trend towards smaller columns to improve mass detectability and increase theoretical plates by column addition, the total volume of the detector has become an important concern. GC does not have a problem of detector cell volume, due to the large peak volumes, however LC peak volumes are much smaller. In order to maintain the resolution of eluting chromatographic peaks, one needs a cell volume one fifth to one tenth of the peak's volume. For conventional packed columns, this would mean a detector volume of 100 µl; microbore columns would require 1 µL; packed microcapillaries would need 0.1 µL; and 10 nL for open microtubular capillary columns (4). Maintaining sensitivity while decreasing volume has been one of the

biggest challenges confronting analytical chemists in developing small detectors. In reducing the volume, quite often the optical pathlength is reduced, and in techniques where sensitivity is proportional to the pathlength, this means a reduction in sensitivity. There is still a need for a universal detector with a volume in the nanoliter range.

An ideal detector should be nondestructive, thus allowing the analyst to combine, in series, a number of detectors allowing one to obtain the maximum amount of information per separation.

The next characteristic to consider is the dynamic range. There are actually two ranges in this characteristic: the linear dynamic range and the dynamic reserve. The former is defined as the concentration range from the minimum detectable to the concentration which causes a five percent deviation from the predicted signal. The latter is a property of detectors which has recently received greater attention. The dynamic reserve is defined as the detector's ability to measure a small change against a large background signal. The reason for the increased interest in this property is the indirect detection schemes (5,6), which allow normally selective detectors to be used as universal detectors.

Although no single LC detector possesses all the properties of an ideal detector, a combination of the many

optical detectors can come close. In recent years, many of the improvements in optical detectors have been achieved by utilizing the unique properties of lasers.

The most familiar property of the laser is its power. Lasers can have substantially greater peak powers and average powers, than conventional light sources. These properties can lead to lower detectability if the signal, but not the noise, increases with laser power.

The second well-known property, collimation, results from the optical cavity which produces coherent light with a well-defined cross-sectional intensity distributions. It is convenient to classify the distributions according to transverse electric and magnetic (TEM) modes which follow a orthogonal series. The simplest of these modes exhibits a Gaussian shaped intensity distribution and is called the TEM_{00}. This lowest mode can be focused to a smaller beam waist than any of the higher modes. Since conventional light source's cross-sectional intensity distributions are linear combinations of lower order TEM modes, light from conventional sources cannot be focused to the same beam waist without sacrificing power.

The monochromaticity of laser beams have proven to be a very useful property. This property reduces scattered light noise in fluorescence measurements; improves the accuracy of results in polarimetry; and reduces baseline instability in

RI measurements due to wavelength drift in the probe light source.

The next property is the temporal resolution of laser beams. Light pulses, as short, as 1×10^{-14} seconds have been produced.

The last property is the ability of laser light to be highly polarized. It has been shown that by taking advantage of collimated beams of small diameters, one can enhance on the rejection ability of polarizing optics (7). Even without special optics to polarize the beam, laser cavity outputs are often polarized. This is due to the polarization of an emitted photon being conserved in stimulated emission and the presence of Brewster's angle windows defining the optical cavity.

From the list of unique properties that lasers possess, it is easy to see why many of the improvements in optical detectors are achieved using these novel light sources.

References

1. Tswett, M. S. Proc. Warsaw Soc. Nat. Sci. Biol. Sect., 1903, 14, minute No. 6.
2. Tswett, M. S. Ber. Deut. Bot. Ges., 1906, 24, 313-26.
3. Tswett, M. S. Ber. Deut. Bot. Ges., 1906, 24, 384-93.
4. Yeung, E. S. In "Microcolumn LC and its Ancillary Techniques"; Novotny, M.; Ishii, D., Eds.; Elsevier:

Amsterdam; in press.

5. Small, H.; Miller, T. E. Anal. Chem., 1982, 54, 462-8.

6. Bobbitt, D. R.; Yeung, E. S. Anal. Chem., 1984, 56, 1577-81.

7. Moeller, C. E.; Grieser, D. R. Appl. Opt., 1969, 8, 206-7.

LASER-BASED SIMULTANEOUS ABSORBANCE, FLUORESCENCE, AND REFRACTIVE-INDEX DETECTOR FOR MICROCOLUMN LIQUID CHROMATOGRAPHY

Introduction

One prominent area of research in the field of liquid chromatography (LC) is the pursuit of smaller diameter columns (1,2). Technology has progressed to the point where packed microcolumns with internal diameters of 1 mm are commercially available, yet technology for many commonly used detectors has not advanced to the same stage. To satisfy this need a number of optical detectors have been developed using both lasers (3-7) and conventional light sources (8,9). Lasers are known to have many advantages applicable to miniaturized optical detectors (10). The advantages of collimation and high power have been used in the development of photothermal (6,7), fluorometric (3), and polarimetric (4,5) detection. The cells for such detectors are either a Z-type with the light shining along the fluid flow or an on-column type with the light propagating perpendicular to the fluid flow. The Z-type cell allows one to have long optical pathlengths thus preserving concentration sensitivity. But, because the effluent stream must flow around two right-angle corners, one may have to deal with additional band broadening. With on-column cells,

one has undisturbed effluent flow, but the pathlength is limited to the width of the column. Thus, when developing a small volume optical cell, one seems to have to make a compromise between band broadening and sensitivity.

In this work, we demonstrate an optical cell in which the light enters the side of the flow stream (similar to the on-column cell) and yet propagates nearly parallel to the flowing stream before reaching the opposite window and exiting. This behavior is accomplished by controlling the incident angle of the light so that it strikes the window-liquid interface at an angle just smaller than the critical angle, thus giving a large angle of refraction. Light incident on an optical interface at an angle just smaller than the critical angle is also very sensitive to changes in the refractive index (RI) of the media making up the interface, and has been recognized as a sensitive means of measuring changes in RI (11). Since it is the change in the refractive indices at the interface which caused the change in light intensity, this mode of detection has the potential for making a very small volume differential refractometer. A cell for RI detection in LC based on transmission near critical angle is in fact commercially available (11). However, it has a volume too large for microbore LC. Furthermore, the transmitted light is detected by back scattering at a second surface. The resulting collection

efficiency is low and the discrimination against the reflection from the first surface is poor. We report here a design based on coupling out the transmitted beam by a second prism, symmetrically placed. A laser source assures a small volume and a high beam intensity. Laser flicker noise is minimized by modulation and a reference flow cell. The pathlength of the optical region is 1 cm with 1-μL volume. This cell further allows the measurement of absorption and fluorescence in the same volume, with pathlengths optimized to maintain good concentration detectability. This combination allows one to obtain the maximum information with the minimum amount of band broadening.

Theory

The behavior of light incident on a dielectric interface, Figure 1, is described by both Snell's law of refraction ($n_1 \sin\theta = n_2 \sin\phi$) and Fresnel's laws of reflection. Fresnel's laws describe the reflection and transmittance of light at an interface for the two types of linearly polarized light. The polarizations are p when the electric vector of light is parallel to the incident plane made by the normal and the incident light ray, and s when the electric vector is perpendicular to the incident plane. The reflection of both polarizations are described by the

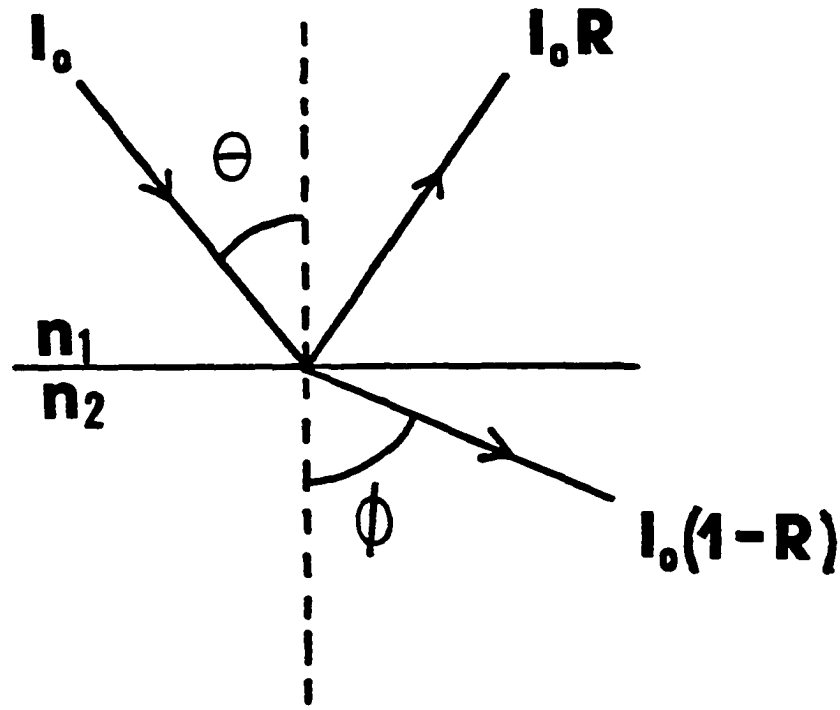

Figure 1. Reflection and transmittance of light at an interface: I_o, incident light intensity; θ, incident angle; ϕ, angle of refraction; n_1, refractive index before interface; n_2, refractive index after interface; R, reflectivity

following equations.

$$R_s = \left[\frac{\cos\theta - \sqrt{(n^2 - \sin^2\theta)}}{n^2\cos\theta + \sqrt{(n^2 - \sin^2\theta)}} \right]^2 \quad \ldots (1)$$

$$R_p = \left[\frac{-n^2\cos\theta + \sqrt{(n^2 - \sin^2\theta)}}{n^2\cos\theta + \sqrt{(n^2 - \sin^2\theta)}} \right]^2 \quad \ldots (2)$$

R_s and R_p are the reflectivities for the s and p polarized light respectively, n is the ratio n_2/n_1, and θ is the incident angle (12).

We found that at an angle as small as 3.6×10^{-3o} from the critical angle of a borosilicate glass ($n_{644nm} = 1.514$) and acetonitrile ($n_D = 1.344$) interface, 10% of the incident light is still transmitted. This is a higher transmittance than is predicted by Eqs. 1 and 2 and is due to the finite angular spread of the beam and also due to imperfections of the interface (13). From Snell's law, one can calculate that such an incident beam will be refracted at the interface to where it makes an angle with the interface of only 0.46^{o}. With this angle and a cell gasket with a thickness of 80 μm, we can conclude that the probe beam propagates 1 cm before exiting the cell.

When calculating the RI of the test mixture, we used the following equation (14)

$$\Delta n = \frac{C_x \left[\frac{n_x^2 - 1}{n_x^2 + 2} - \frac{n_e^2 - 1}{n_e^2 + 2} \right]}{6n_e/(n_e^2 + 2)^2} \quad \ldots (3)$$

In Eq. 3, Δn is the change in RI, C_x is the volume fraction of the analyte, and n_x and n_e are the RI of the analyte and the eluent. We have found this equation to give a more accurate description of the RI of nonpolar mixtures (14) compared to calculations based on a linear interpolation of the RIs for the two components in the mixture (15).

Experimental

RI and absorbance detector

The experimental arrangement to detect both RI and absorbance change is shown in Figure 2. A helium-neon (HeNe) laser (Melles Griot, Irvine, CA, Model 05-LHR-151 and 05-LPL-340) is modulated between the two flow cells by a acoustooptic light modulator (Bragg cell, Coherent Associates, Danbury, CT, Model 304 and 305D) which is driven by a signal generator (Wavetek, San Diego, CA, Model 162) at 100 kHz. A 50-cm focal-length lens focuses the beam into the optical cell. An optical flat is used to balance the intensities of the two beams reaching the detector, based on the variation in natural reflection with angle and with polarization. After passing through the cell, light is

Figure 2. Absorbance and refractive index detector and chromatographic system: PU, pump; INJ, injecter; CM, microbore column; LASER, helium-neon laser; L, lens; MOD, Bragg cell modulator: OF, optical flat; CELL, optical cell; PD, photodiode: DR, driver; SIG, signal generator; LI, lockin amplifier; PDP/11, minicomputer; SC, strip chart recorder; OSC, oscilloscope

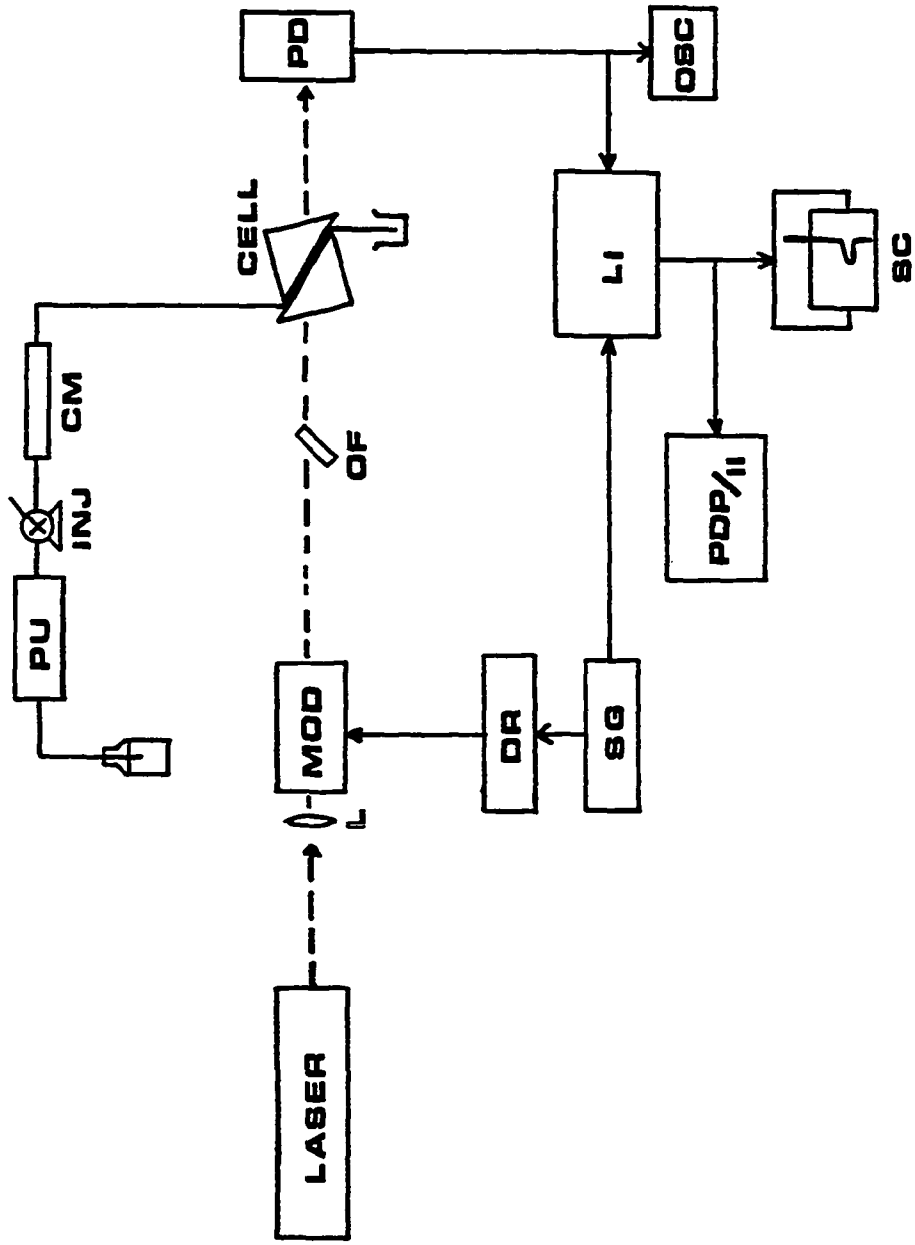
PD
OSC
CELL
LI
SC
CM
OF
INJ
PDP/11
PU
MOD
DR
SG
LASER

detected by a photodiode (Hamamatsu, Middlesex, NJ, Model S1790). The output from the diode is sent into either an oscilloscope (Tektronixs, Beaverton, OR, Model 7904) or a lockin amplifier (Princeton Applied Research, Princeton, NJ, Model HR-8). The oscilloscope was used to optimize the modulation of the Bragg cell and the lockin amplifier converts the modulated signal to a DC signal with a 3-s time constant, which is in turn sent to both a strip chart recorder (Houston Instruments, Austin, TX, Model 5000) and a minicomputer (Digital Equipment, Maynard, MA, Model PDP 11/10 with LPS-112 laboratory interface) for data collection.

The 100-kHz high-frequency modulation allowed us to improve the intensity stability of the laser (i.e., lowering the "flicker noise") from a noise-to-signal (N/S) ratio of 5 x 10^{-3} to 2 x 10^{-5}. With the cell placed in the beam and adjusted to 20^{o} less than the critical angle, we still have an intensity stability, N/S, of 2 x 10^{-5}, but with the cell adjusted near the critical angle (allowing 10% of the light to be transmitted) we see an increase in noise, making the N/S ratio 2 x 10^{-4}. This increase in noise is caused by the beam being partially clipped by the optical beam aperture of the glass-liquid interface. Naturally, the decrease in pathlength and in the ΔRI sensitivity when one moves away from the critical angle makes it necessary to operate close

to the critical angle despite a poorer N/S ratio.

Fluorescence detector

The experimental arrangement to detect fluorescence is shown in Figure 3. An argon ion laser (Control Laser, Orlando, FL, Model 554A) was used at 488 nm as the excition source. The best detectability was found for the beam unmodulated. The 50-cm lens focused the laser beam into the cell. A photomultiplier tube (PMT, Hamamatsu, Middlesex, NJ, Model R928) operated at -500 V by a power supply (Cosmic Radiation Labs, Bellport, NY, Model 1001B Spectrastat) was placed above the optical path of the transmitted beams and as close to the cell as possible. Three 540 nm line filters and one colored glass filter (Corning Glass, Corning, NY, Model 3-69) were used to block the excitation light and reduce the background emission from the prisms. The output from the PMT was sent into a picoammeter with current suppression (Keithley, Cleveland, OH, Model 417 and 4170) and with a 3-s time constant. The output from the picoammeter was sent to both the strip chart recorder and the computer for data collection.

Chromatography

All reagents and eluents used are reagent grade material without further purification. The water is deionized and purified by a commercial system (Millipore, Bedford, MA, Milli-Q System). The chromatographic system

Figure 3. Fluorescence detector and chromatographic system: PS, power supply; LASER, argon ion laser; PMT, photomultiplier tube; PA, picoammeter; other symbols as in Figure 2

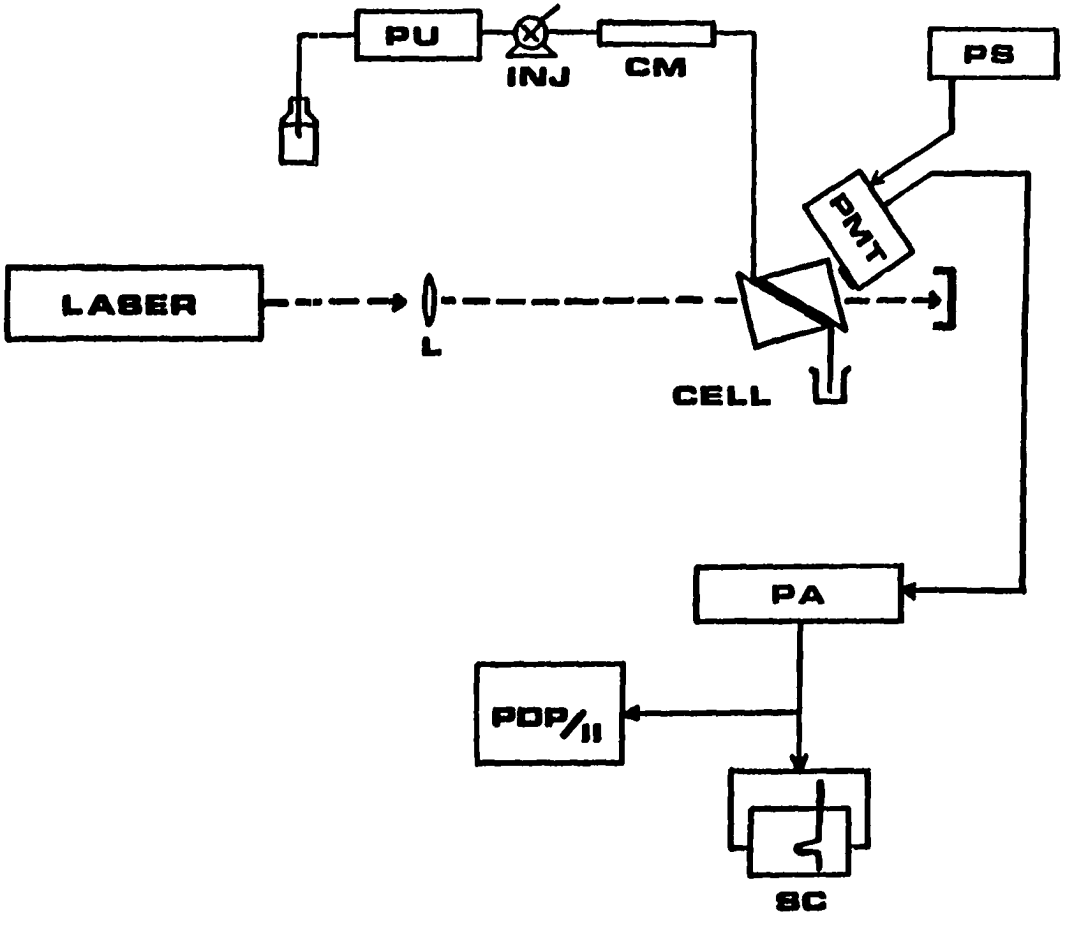
PU
INJ
CM
PS
PMT
LASER
L
CELL
PA
PDP/11
SC

consisted of a syringe pump (ISCO, Lincoln, NE, Model 314), a 0.5-μL sample loop coupled to an internal loop injection valve (Rheodyne, Berkeley, CA, Model 7410) and a 25-cm x 1-mm 5-μm microsphere C_{18} chromatography column (Alltech, Deerfield, IL). All eluents were degassed under vacuum by using ultrasonic agitation.

Cell

The cell consists of a teflon tape gasket squeezed in between two high quality right-angle prisms (Oriel, Stamford, CT, Model 4607), as shown in Figure 4A. The teflon tape defines the flow channels for both the reference and sample chambers as shown in Figure 4B. The inlet and outlet tubes are made of 1/16 in. O.D. stainless steel tubing and are filed down to a wedge at the cell end to minimize dead volume. The connecting tubing between the column and the optical region is 4 cm long with an inside diameter of 0.004 in. The other three tubes (outlet to the sample chamber and inlet and outlet to the reference chamber) have inside diameters of 0.010 in. Epoxy (Armstrong Products, Warsaw, IN, Adhesive A-12) sealed the tubes to the prisms, while braces held the tubes rigidly and minimized the danger of breaking the seal due to accidental bumping. The prisms are pressed together by additional braces placed at the apex of each. This homemade assembly was mounted in a rotation stage (Aerotech, Pittsburgh, PA,

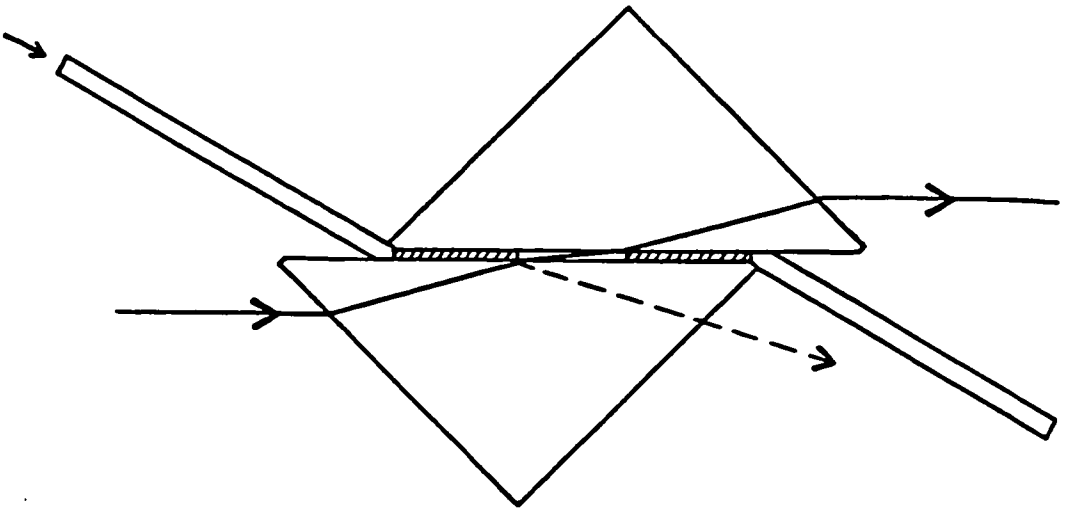

Figure 4A. Side view of optical cell

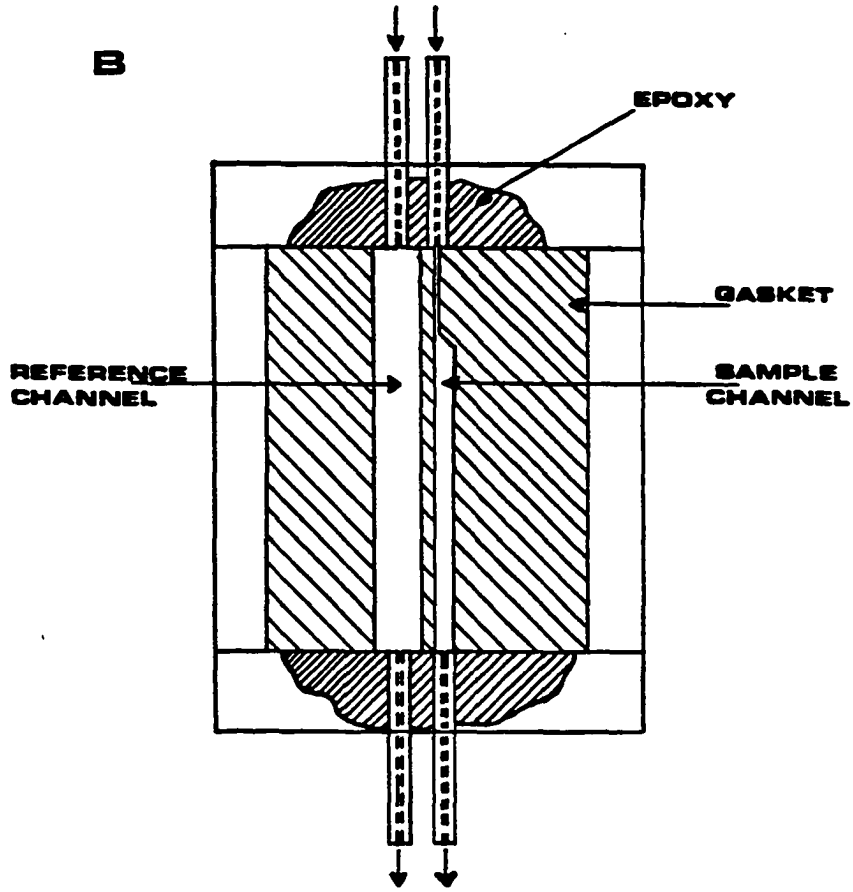

Figure 4B. Top cutaway view of optical cell

Model ATS-301R) with a resolution of 10^{-3o}. The sample channel, Figure 4B, was 1 mm wide when used with the argon ion laser and 2 mm wide in the optical region with the HeNe laser. The reason for the different widths is that the argon ion laser can be focused to half the beam waist of the HeNe laser for the focal-length lens. For a 1 cm optical pathlength (the actual length of the channel), a 80-μm thick gasket, and a 1-mm wide flow channel, the cell has a optical volume of 0.8 μL.

It is possible to make an even smaller cell. The easiest way would be to reduce the thickness of the gasket. Another way is to eliminate the small-bore connecting tubing between the cell and the column, which is adding 0.51 μL to our total cell volume. This was not possible here since the particular microbore column requires an end fitting to be held in place by a chromatographic union at the end of the column. The last possibility is to use a shorter focal length lens to focus the beam to a smaller beam waist, thereby allowing one to make a narrower flow channel. The ultimate size of the beam waist depends on the desired pathlength through the liquid, as has been discussed earlier (10).

Results and Discussion

RI detector

The test mixture was chosen to be benzene diluted in acetonitrile. Solutions were prepared by successive dilutions with no greater than 100 fold for each to minimize dilution errors. Figure 5 shows a chromatogram of benzene being eluted by the acetonitrile eluent at a flow rate of 30 μL/min. The dip before the peak is due to an unidentified impurity and does not add to the peak height or area. 0.5 μL of 5×10^{-4}(v/v) benzene in acetonitrile was injected to obtain this peak. The RI of the test solution was calculated by using Eq. 3 with the RI of benzene and acetonitrile being $n_D = 1.501$ and $n_D = 1.344$, respectively. Taking into account the dilution to a peak volume of 3 μL, this peak shows a detectability of 2.0×10^{-7} RI units (R.I.U., S/N = 3, with noise = one standard deviation). This is comparable to the detectability of commercial RI detectors. The detectable mass of injected benzene is however only 6 ng, which shows the advantage of using microbore columns for increased mass detectability. The chromatogram also shows the high number of plates possible with a microbore column, 78,000 plates/meter in this case with $k' = 1.2$. It should be noted that since the peak has a volume of only 3 μL and since commercial RI detectors have cells with optical volumes of approximately 10 μL (with

Figure 5. Refractive index chromatogram of benzene: Peak is 370 ng of benzene

total volumes much larger), the peak could not have been detected properly with any presently available RI detector without severe band broadening.

When optimizing the detector, questions arise such as what is the best angle to set the liquid-glass interface with respect to the critical angle, and how critical is the placement of the cell with respect to the focal point of the lens. Although Fresnel's equations predict the change in transmitted light per change in ΔRI to increase as one approached the critical angle, the fractional flicker noise in the transmitted beam also increases. We found the optimum setting for ΔRI detection to be that with 10% of the incident beam being transmitted and occurs 0.004 degrees from the critical angle. At this angle, the transmitted intensity for s versus p polarized light differ by less than a percent, therefore one will lose very little sensitivity by having randomly polarized light. Although the radius of curvature of the wavefront of a focused Gaussian beam goes to infinity at the focal point, we did not see a noticeable difference in S/N due to working at the focal point versus slightly away from it. Our choice of a 50-cm focal-length lens is a compromise between the beam waist, which increases with increased focal lengths (thus requiring larger cell volumes), and the curvature of the wavefront, which decreases with increasing focal lengths, to give greater

S/N.

In addition to being able to use a HeNe laser and Bragg cell as a modulated light source, we also were able to use an argon ion laser, modulated by an electrooptic light modulator (Pockels cell, Lasermetrics, Teaneck, NJ, Model 3030). This device was driven by a high frequency power supply (Conoptics, Danbury, CT, Model 25) triggered by a signal generator in the square wave mode. A beam displacer (Karl Lambrecht, Chicago, IL, Model MBDA10) separated the two polarized beams produced by the Pockels cell. We found this latter setup to also give low flicker noise (N/S = 2 x 10^{-5} without the cell) and equally good detectability (Δn = 3 x 10^{-7} R.I.U.).

Absorbance detector

In order to test the ability of the system to measure absorption, one needs a sample compound with a high molar absorptivity, so as to be certain that the analyte peak is at such a low concentration that a ΔRI peak is not observed instead. The test compound chosen was bromocresol green, an organic dye commonly used as a titration indicator. At the HeNe laser wavelength of 632.8 nm, we measured its molar absorptivity to be ε = 31,000 L/moles-cm. Figure 6 shows a chromatogram of bromocresol green being eluted by an eluent of 3:1 methanol in an aqueous buffer of 1 mM citric acid at pH = 7.4 at a flow rate of 30 μL/min. Since bromocresol

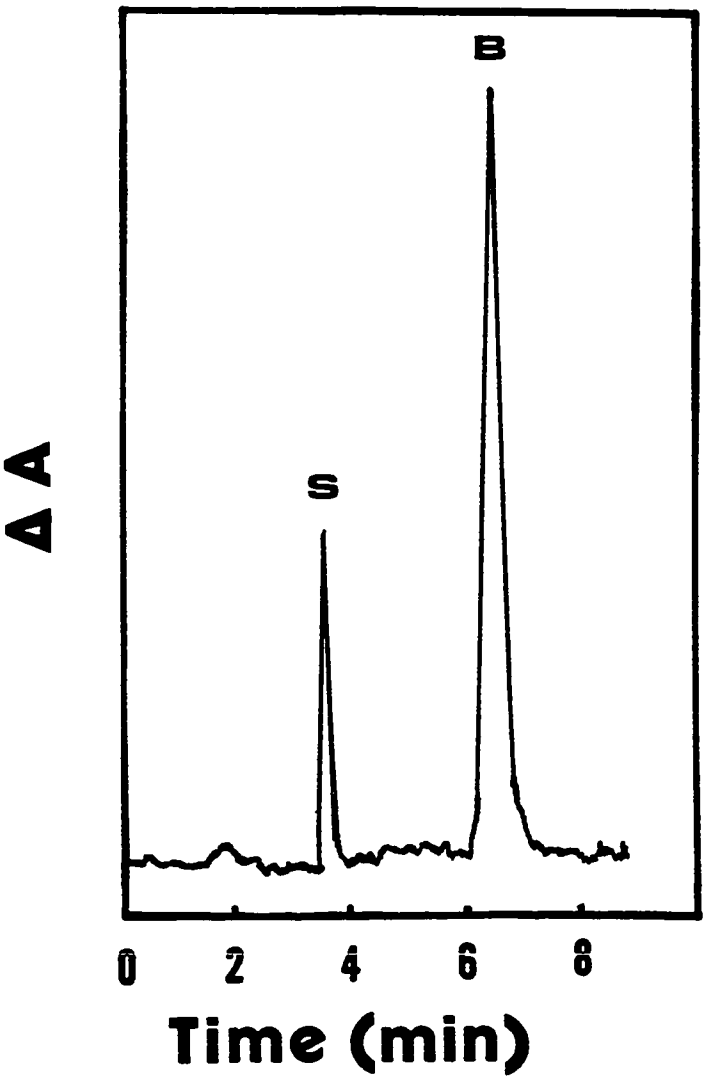

Figure 6. Absorbance chromatogram of bromocresol green: S, solvent peak; B, 3.5 ng of bromocresol green

green is a weak acid with a pK_a = 4.7 it is easily protonated in low pH solutions. At pH = 7.4, we have 99% in the unprotonated form. In the chromatogram the first peak is a solvent peak detected as a RI change. The second peak is 0.5 μL injection of 9.9×10^{-6} M bromocresol green showing an absorbance detectability of 2.1×10^{-4} A.U. (S/N = 3). This compares well with the 2.2×10^{-4} A.U. detectability value one can calculate from the flicker noise of $N/S = 1.7 \times 10^{-4}$. The mass detectability corresponds to 48 pg of injected bromocresol green. It should be pointed out that a peak detected by absorbance will decrease the intensity of the probe beam, whereas a peak due to ΔRI will increase the intensity of the probe beam for an increase in RI. Since the LC eluent can be chosen to have a small RI, one can assure that ΔRI is always positive. So, one can distinguish a RI peak from an absorbance peak. If a species produces both a RI peak and an absorption peak, reduced sensitivity will be obtained due to partial cancellation.

Initially, we felt that since we have a RI detector, we could also make a very sensitive absorbance detector by taking advantage of the photothermal effect (16) seen in techniques such as thermal lens and photothermal diffraction. The photothermal effect allows one to measure absorbance indirectly by measuring the change in RI of the sample due to heating by a high-intensity excitation beam.

A test of excitation beams from 1 to 100 mW gave enhancements of only about 30% of the peak height for bromocresol green. The reason for this discrepancy is that only the RI at the glass-liquid interface is monitored. Even though the bulk liquid may be heated by the absorption event, the interface is at a substantially lower temperature because of cooling (by conduction and by flow). One can estimate the linear flow velocity of the eluent to be 0.625 cm/s in the cell. Even with a 100-μm beam waist, the residence time of the liquid in the beam is only 0.016 s, too short to establish a thermal effect at the interface. So, this detection cell is not suitable for photothermal measurements, but is expected to show less thermal drift for RI measurements compared to other detection schemes.

Fluorescence detector

The best detectability was achieved in the fluorescence mode with a picoammeter monitoring the phototube current and not with a lockin amplifier with modulation. It was observed that the prisms used to make up the cell give off luminescence with a lifetime of several milliseconds. This is probably due to trace amounts of rare earth ions in the borosilicate glass giving off phosphorescence. Measurement of the fluorescence from the test solution was tried with modulation at frequencies much faster than the luminescence lifetime (100 kHz), but poor flicker noise in the

luminescence background was observed. Slower modulation (100 Hz) was also tried, but again failed to give improved detectability over detection with a picoammeter. This however still allows the cell to be used simultaneously for fluorescence, RI, and absorption. The excitation beam is modulated as described above for RI and absorption, and these are monitored with a photodiode through a lockin amplifier. The phototube for fluorescence detection is simply connected to a picoammeter without demodulation.

The test molecule was a highly fluorescent compound formed by derivatization of propylamine by 7-chloro-4-nitrobenzo-2-oxa-1,3-diazole (NBD-Cl). Figure 7 is a chromatogram of propylamine-NBD being eluted by 3:1 methanol in water at a flow rate of 33 μL/min. The peaks before the fluorescence peak are reproducible injection disturbances which are also seen when the methanol solvent is injected. The injected solution was a 1.2×10^{-6} M solution of propylamine-NBD with 9 fold excess of NBD-Cl. The unreacted NBD-Cl has a very small fluorescence quantum yield and elutes after the propylamine-NBD peak. The analyte peak shows a detectability of 0.8 pg (S/N = 3). We note that if there is a large RI change, the pathlength will change and the fluorescence intensity will be affected. However, at the typical low concentrations in fluorescence detection, RI changes are small. This type of potential interference is

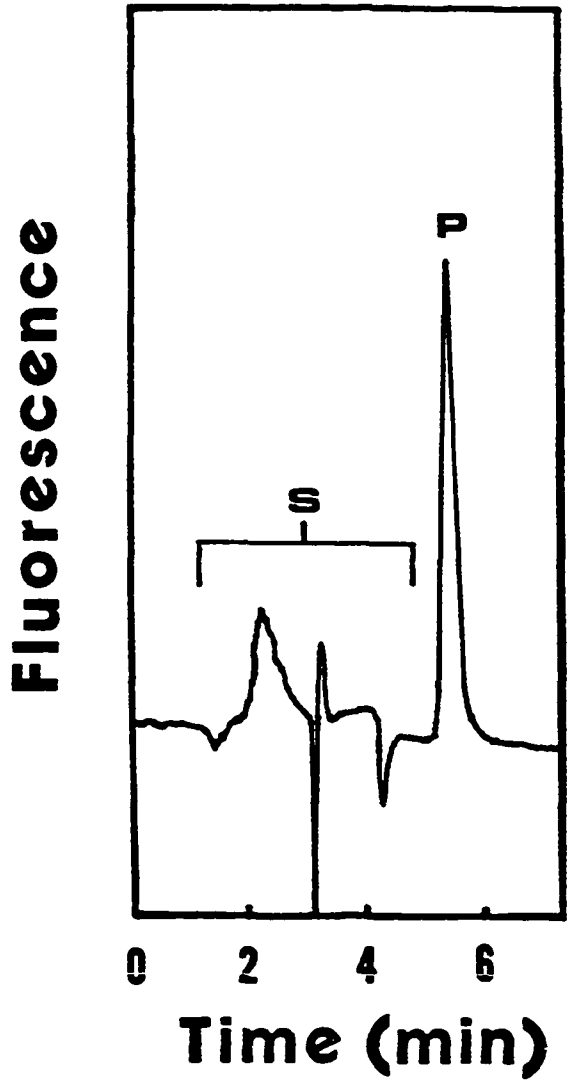

Figure 7. Fluorescence chromatogram of derivatized product of propylamine and NBD-Cl: S, reproducible injection disturbance; P, 125 pg of fluorescent propylamine derivative. Excess NBD-Cl elutes after the propylamine derivative and was not detected

thus expected to be less common than in the case of absorption detection.

Conclusion

In summary, we have demonstrated a novel optical cell which has a volume small enough for microcolumn LC and which allows one to monitor an effluent stream by three different modes of detection. Individually, the detectabilities of RI, absorption, and fluorescence are comparable to, but not superior to, those obtained from cells specifically designed for each detection mode. However, this detection method uses the same optical region, so one obtains the maximum amount of information with the minimum amount of band broadening. The limiting factors here are laser flicker noise and alignment instabilities, and future improvements should be possible if these can be reduced.

References

1. Novotny, M. Anal. Chem. 1981, 53, 1294A-1308A.
2. Yang, F. J. High Resol. Chromatogr. Chromatogr. Comm. 1983, 6, 348-58.
3. Folestad, S.; Johnson, L.; Josefsson, B.; Galle, B. Anal. Chem. 1982, 54, 925-9.
4. Bobbitt, D. R.; Yeung, E. S. Anal. Chem. 1984, 56, 1577-81.

5. Bobbitt, D. R.; Yeung, E. S. Anal. Chem. 1985, 57, 271-4.

6. Buffett, C. E.; Morris, M. D. Anal. Chem. 1983, 55, 376-8.

7. Sepaniak, M. J.; Vargo, J. D.; Kettler, C. N.; Maskarinec, M. P. Anal. Chem. 1984, 56, 1252-4.

8. Yang, F. J. High Resol. Chromatogr. Chromatogr. Comm. 1981, 4, 83-5.

9. Hibi, K.; Ishii, D.; Fufishima, I.; Takeuchi, T.; Nakaniski, T. High Resol. Chromatogr. Chromatogr. Comm. 1978, 1, 21-7.

10. Yeung, E. S. In "Microcolumn LC and its Ancillary Techniques"; Novotny, M.; Ishii, D., Eds.; Elsevier: Amsterdam, 1985; p. 135-58.

11. Watson, E. S. Amer. Lab. 1969, 1, 8-12.

12 Fowles, G. R. "Introduction to Modern Optics", 2nd ed.; Holt, Rinehart and Winston: New York, 1968; p. 44.

13. Ding, T. N.; Garmire, E. Appl. Opt. 1983, 22, 3177-81.

14 Synovec, R. E.; Yeung, E. S. Anal. Chem. 1983, 55, 1599-1603.

15. Skoog, D. A.; West, D. M. "Principles of Instrumental Analysis", 2nd ed.; W. A. Saunders: Philadelphia, PA, 1980; p. 374.

16. Woodruff, S. D.; Yeung, E. S. Anal. Chem. 1982, 56, 1174-8.

LASER-BASED DIFFERENTIAL ABSORBANCE DETECTOR USING MICHELSON INTERFEROMETRY

Introduction

In liquid chromatography, the absorbance detector is the most commonly used detector, due to its sensitivity and selectivity (1). Commercial absorbance detectors have detection limits on the range of 10^{-3} to 10^{-4} absorbance units (A.U.), and work on the principle of measuring a change in the intensity of light transmitted through a sample. In the last few years, a number of indirect absorption techniques have demonstrated improvements in the detection limit down to the absorbance range of 10^{-6}, using the unique properties of lasers. These techniques are called indirect, because rather than measuring a change in the intensity of transmitted light, they respond to heating of the sample by light being absorbed. Thermal lens calorimetry, for example, measures the effect on the probe beam of nonuniform heating in the sample caused by absorption of an intense laser beam (2). A technique developed by Stone (3,4) is the measurement of the bulk heating of a sample by absorption of an intense laser beam. Absorption is detected by observing a change in the optical pathlength inside an interferometer. The limitation in the two technique's detectability is due to background

absorbance of the solvents used to make up the solutions. Solvents such as methanol or water, which are transparent in the visible region, actually absorb in the range of 10^{-3} to 10^{-4} A.U. due to vibrational overtones (5-7). To improve on the 10^{-6} A.U. detection limit, one must either improve the precision of the present methods or find differential indirect absorption techniques which prevent one from having to measure a small change in absorbance against a relatively large background absorbance.

Such differential techniques have recently been shown for the photothermal techniques of thermal lens calorimetry (8) and the technique described earlier based on phase change in an interferometer due to sample heating in absorption (9). The differential thermal lens technique takes advantage of the different responses when the sample cell is placed before the focal point of the probe beam or after. When the cell is placed before the focal point, the thermal lens in the cell will diverge the beam at the photodetector; when placed after the focal point the beam will be focused into the photodetector. The two responses will cancel the effect of absorption in each cell with proper placement, allowing only the difference in absorbance to be seen. In the second differential technique, an additional set probe beams were added to Stone's setup which allowed the fringe pattern formed by the two primary probe

beams to be stabilized while passing through two different cells. If the cells absorb equally, then they will have equal optical phase change and the resultant phase change will be zero. But if one cell contains an analyte which absorbs, the resultant phase change will not be zero.

In this work, we describe a third differential technique which also uses interferometry. In this technique's simplest form, the two cells (one containing the solvent and the other containing an analyte in the solvent) would each be placed in a beam of a two beam interferometer. The two beams would be recombined after the cells with the phase difference adjusted to where they destructively interfere. Ideally, with no absorbance in the cells, the interference would be complete and no light would be output from the interferometer. When the cells have equal absorbance, one would have equal decrease in the transmitted light and the beams would again produce no output. Only in the case of unequal absorbance between the two cells would light be output by the interferometer. This technique would have at least two advantages over the other differential techniques. First, it is conceptually very simple, and second, it is a nonphotothermal technique, thus not requiring a high intensity light source. A disadvantage is that a high quality destructive interference will be hard to achieve and maintain.

A subtle point is that this technique could allow a reduction in a light source's intensity instability ("flicker noise"). This is achieved by reducing the background light levels by destructive interference, thus reducing the flicker noise from the light source.

There are two general types of interferometers; they are division of amplitude and division of wavefront. In the former type, the light is split into two beams by a partially reflecting surface (i.e., a beam splitter) dividing the amplitude of the wave, but not the wavefront. In the latter, the beam is split into two or more beams by apertures dividing the wavefront (such as in the classical Young's double slit experiment). Of the two types, the division of amplitude interferometer should give the best destructive interference, since the two beams intensity profile will originate from the same points in the source. Therefore, there would be greater coherence of the two beams compared to two beams which come from different points in the source. Not only will the phase be closely correlated, but any amplitude fluctuations will also be correlated. The simplest division of amplitude interferometer is the Michelson interferometer (10,11) which is shown in its simplest form in Figure 1.

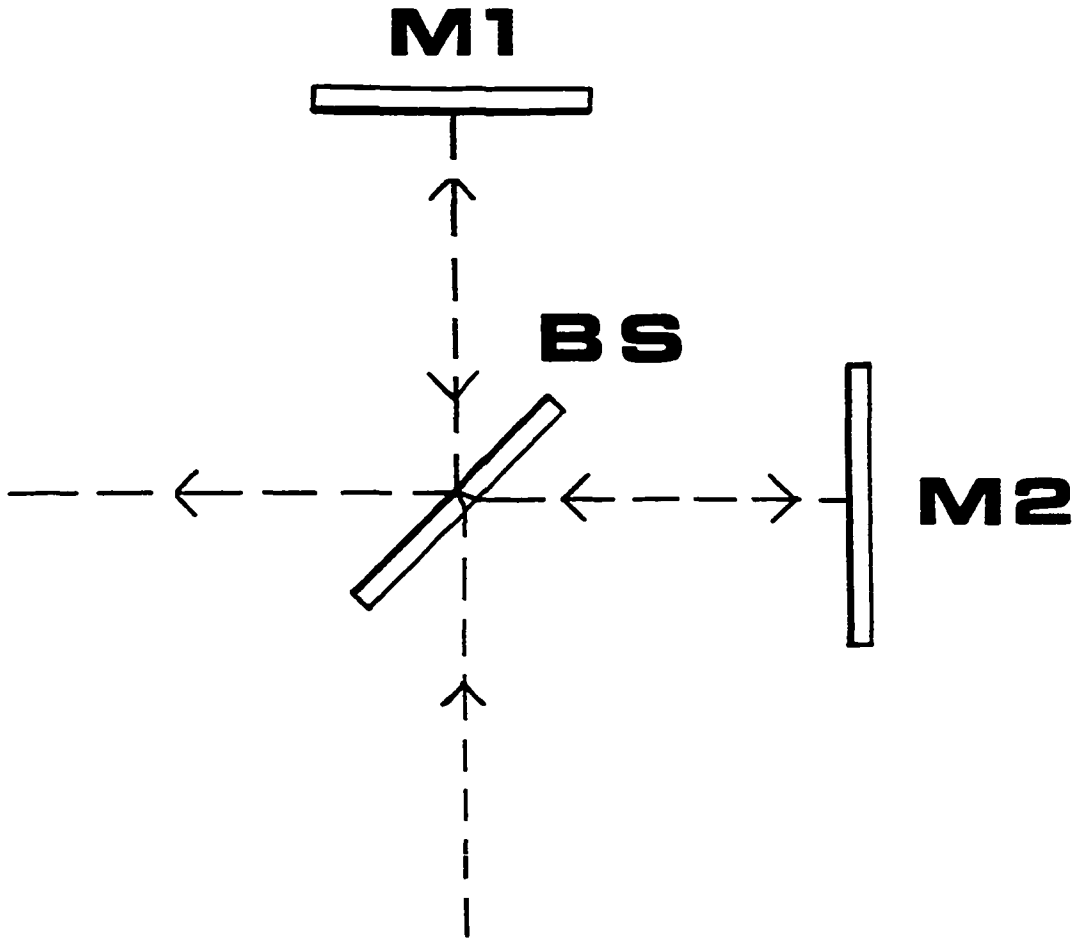

Figure 1. Optical diagram of a Michelson interferometer: M1 and M2, high quality interferometer mirrors; BS, beam splitter

Theory

For this technique to work one must achieve a very complete destructive interference. The easiest way to compare the quality of destructive interferences is to use a ratio of the intensity of light at minimum output, I_d, versus maximum output, I_c. We shall call this the extinction ratio, E_x; defined as

$$E_x = I_d/I_c. \qquad \ldots (1)$$

In a Michelson interferometer, the entering light strikes a partially reflecting surface causing the light to be split into two beams. When the two beams are reflected back onto the partially reflecting surface by mirrors, they form an output beam which is a superposition of the two beams. When a coherent light source is used, this superposition of the two light beams gives rise to interference. The resultant amplitude, E, of the two superposed light beams is the sum of the amplitudes of the individual waves, E_1 and E_2, so

$$E = E_1 + E_2 \qquad \ldots (2)$$

The intensity of a light wave, I, is given by

$$I = (c/4\pi) \sqrt{(\varepsilon/\mu)} \langle E^2 \rangle \qquad \ldots (3)$$

where c is the speed of light in a vacuum, ε is the dielectric constant, μ is the magnetic permeability (12). Since the comparison of I is in the same medium, the quantity $\langle E^2 \rangle$ is a measure of the intensity.

To obtain the intensity of two interfering light beams, one must take the square of the sum of the amplitudes of the two waves,

$$I \propto \langle E^2 \rangle = \langle (E_1+E_2)^2 \rangle . \quad \ldots (4)$$

Multiplying, one obtains

$$I \propto \langle E_1^2 + E_2^2 + 2E_1E_2 \rangle \quad \ldots (5)$$

where the last term is called the interference term. The amplitudes can be replaced by the individual beams intensities, if the phase difference of the interfering waves is taken into account by adding a cosδ, where δ is the phase difference between the two waves.

$$I = I_1 + I_2 + 2\sqrt{(I_1 I_2 \cos\delta)} \quad \ldots (6)$$

The effect on the output of the interferometer by an absorption in one arm is predicted by an equation formed by combining Eq. 6 and Beer's law. The form of Beer's law which describes the attenuation of light by absorbance is

$$I_T = I_0 10^{-A}, \quad \ldots (7)$$

where I_T is the light transmitted through the sample, I_0 is the incident light, and A is the absorbance of the sample. Substituting Eq. 7 into Eq. 6 with $I_2 = I_0$, one obtains

$$I = I_1 + I_2 10^{-2A} + 2\sqrt{(I_1 I_2 10^{-2A})}\cos\delta \quad \ldots (8)$$

where 2A is used instead of A because the beam passes through the sample twice. We also make the assumption of very small A, so that I_0 may be used as the incident intensity for each pass instead of I_0 and then $(1-10^{-A})I_0$.

Since in a Michelson interferometer each beam is both reflected and transmitted once by the partially reflecting surface, the output intensity from each arm is the same (for the case of no absorbance in each arm and perfectly reflecting mirrors), therefore $I_1=I_2$. When the beams are half a wavelength out of phase, one has destructive interference and $\cos\delta=-1$. This leads to the simplified equation of

$$I = I_1(1 + 10^{-2A} - 2x10^{-A}) \qquad \ldots (9)$$

Making the substitution of $A=\varepsilon bc$, where ε is the molar absorbtivity, b is the pathlength, and c is the concentration in moles/liter, one obtains

$$I = I_1(1 + 10^{-2\varepsilon bc} - 2x10^{-\varepsilon bc}). \qquad \ldots (10)$$

Using Eq. 9 we can calculate how small of a extinction ratio we will need in order to detect a change in absorbance of 10^{-7}. By substituting in for A, we calculate a change in the transmitted light of $5.3x10^{-14}$. Even with a source intensity stability (i.e., flicker noise) of one percent, we will still need a extinction ratio of $5.3x10^{-12}$.

Experimental

The Michelson interferometer, used to test for the best possible extinction ratio, was built using parts from a commercial Fabry-Perot interferometer (Burleigh, Fisher, NY, Model RC-100 with RC-670-C2.3 mirrors). There are several

advantages to using parts from a commercial interferometer, such as excellent thermal stability, rigid mirror mounts with high precision micrometers, and high quality mirrors. This commercial interferometer is made with all Super-invar alloy for excellent thermal and mechanical stability. Super-invar is an alloy consisting of Ni-Fe-Co with 30-64-6 wt.% respectively and has been found to have very low thermal expansion (α=0.36x10^{-6}/^{o}C) near room temperature (13). The other parts to the interferometer were made of iron which has the lowest thermal expansion for common metals (α=12.x10^{-6}/^{o}C, Ref. 14). The Fabry-Perot interferometer has two mirrors with the faces parallel to each other. One mirror is on a sliding mirror mount on rails and the other is on a fixed mirror mount which holds the rails. To make a Michelson interferometer, one needs the mirrors placed roughly perpendicular to each other. We were able to convert this interferometer by building a rail holder to replace the end mirror mount and moving the now freed mirror mount to a position allowing us to have roughly perpendicular mirrors. An iron mount was built to hold the beam splitter allowing us to rigidly position it opposite the rail mounted mirror. To prevent distortions, epoxy (Armstrong Products, Warsaw, IN, Adhesive A-12) was used to hold the beam splitter onto the mount.

The light source was a single-frequency helium-neon

(HeNe) laser which was directed into the interferometer by two adjustment mirrors as shown in Figure 2. An aperture was placed before the first adjustment mirror to clean up the beam. A quarter-wave plate (Oriel, Stamford, CT, Model 2562) converted the polarized light from the laser into circularly polarized light. Then, a Glan prism (Karl Lambrecht, Chicago, IL, Model MGT-25E8-45) held in a rotational stage (Aeroteck, Pittsburgh, PA, Model ATS-301R) repolarized the light, thus giving us the same intensity of polarized light at any chosen angle. In order to balance the intensity in each arm of the interferometer, the mirror in the free standing mount was reversed so that a small amount of light was lost due to reflectance from the air-substrate interface. Then, the polarization of the input beam was rotated so that a varying amount of light was lost in the second arm of the interferometer at the uncoated surface of the beam splitter.

The output of the interferometer was sent into a photomultiplier tube (Amperex, Hicksville, NY, Model 56TVP) operated at -2000V by a high-voltage power supply (Hamner Electronics, Princeton, N.J., Model NV-13-P). Two 632.8-nm interference filters (Corion, Holliston, MA, Model 30-6328-1) were used to reject room light. The phototube's output was sent into either a photon counting system (Ortec, Oak Ridge, TN, Model 9302 and 9315) or a digital multimeter

Figure 2. Block diagram of equipment used to test for lowest output from Michelson interferometer: L, single-frequency HeNe laser; M3 and M4 aluminum coated mirror; OF, optical flat; QW, quarter-wave plate; P, polarizer; F, neutral density filters; LF, two interference filters; PMT, photomultiplier tube; PS, power supply; PC, photon counting system; DMM, digital multimeter; REC, strip chart recorder; OP, high-voltage operational amplifier; SG, signal generator; FVS, floatable voltage supply; VVS, variable voltage supply

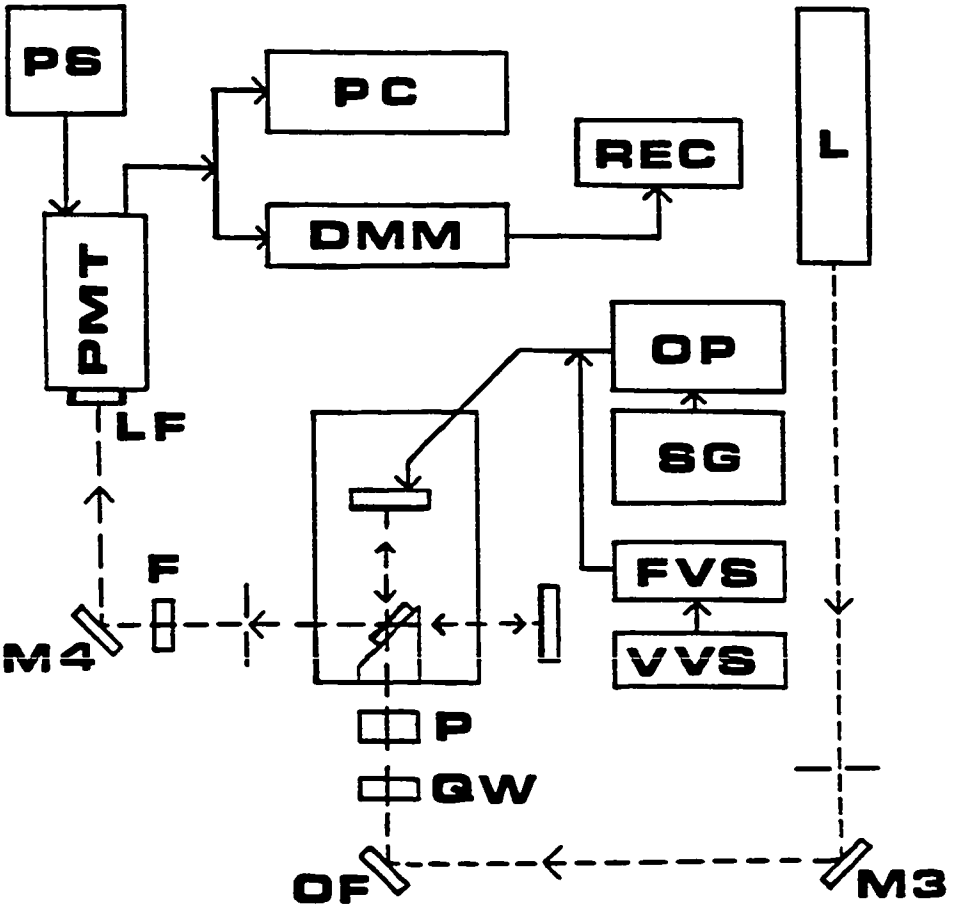
PS
PC
REC
L
DMM
PMT
OP
LF
SG
F
FVS
M4
VVS
P
QW
OF
M3

(Keithley Instruments, Cleveland, OH, Model 160b/1602B). A strip chart recorder (Measurement Technology, Denver, CO, Model CR452) measured the output from the multimeter and was useful in recording the minimum phototube current, thus finding the optimum alignment. The optimum alignment was found by viewing the fringe patterns from the interferometer on an index card. Crude alignment was obtained first by aligning with the mechanical micrometers and then fine adjustment of the mirrors was accomplished using piezoelectric pushers in the rail mounted mirror. The adjustment voltages to the piezoelectric pushers came from a variable voltage power supply (Tropel, Fairport, NY, Model PZM) with a homemade floating voltage supply allowing extra fine adjustments. The rail mounted mirror could also be translated, to adjust the phase of the light in one arm, by adjusting the bias on a high voltage operational amplifier (Burleigh, Fisher, NY, Model 162). Finding the optimum alignment was facilitated by viewing the fringe pattern, while a saw-tooth wave generator (Wavetek, San Diego, CA, Model 162) drove the operational amplifier which powered the piezoelectric pushers. For rigidity, the interferometer was fastened down to a optical table (Newport Research, Fountain Valley, CA, Model LS-48) which was floated on air by a pneumatic isolation system (NRC, Fountain Valley, CA, Model XL-B/A). Floating the table on air allowed us to minimize

the effects due to vibration of the optics. The extinction ratio was measured with the photon counting system using neutral density filters (Melles Griot, Irvine, CA, Model 03-FSG-017) to reduce the intensity of the output to a level which does not saturate the phototube.

Results and Discussion

From the theory section, we saw that a very small extinction ratio of 5.3×10^{-12} would be needed to see a difference on absorbance between the two cells of 10^{-7}. The lowest ratio that we were able to obtain was 2×10^{-5}. This ratio will only allow us to see a change in the 10^{-4} A.U. range, assuming again that we have 1% flicker noise.

In searching for the reason for the high extinction ratio, one could start by recalling the conditions needed for a complete destructive interference, thus a very low extinction ratio. One would need uniform pathlength, the same polarization in both beams, and equal amplitudes between each overlapping point in the two beams.

The pathlength requirement is of course needed to have the phase be equal across the superposed beams, so that one point in the output beam isn't at the minimum while an other is slightly away from it. This puts strict requirements on the mirror's flatness and even though these are state-of-the-art, they are quoted as having a flatness of only one

two-hundredth of a wavelength. Therefore, at best, they will cause a nonuniformity in the pathlength of twice that or one hundredth of a wavelength (or fringe). It should be noted that we observed severely distorted fringe patterns output by the interferometer when a one-eighth-inch-thick beam splitter was clamped into a metal mount. This was attributed to distortions of the beam splitter caused by the mounting, because when a second identical beam splitter was epoxied onto the mounting block, no distortions were seen.

The polarization conditions are as equally hard to achieve. First, note that waves of orthogonal polarization do not interfere, so any rotation of one of the beams would create a noninterfered-with electric field vector. In the building of a laser-based polarimeter by Yeung and coworkers, it was found that an extinction ratio of 10^{-10} was possible with a laser light source sent through carefully selected spots on crossed Glan prisms (15). They also found that any high quality optical flat placed in the beam supplied sufficient birefringence to depolarize the beam to a level which caused an extinction ratio of only 10^{-5}. Because our polarization requirements are equally as strict and we must use an optical flat as a substrate to our beams splitters, lack of meeting this condition would seem to be a major problem. In an effort to minimize the birefringence conditions, the beam splitter on the

one-eighth-inch-thick substrate was replaced by a pellicle-type beam splitter (Oriel, Stamford, CT, Model 3743). This substrate had a thickness of only 7μm, so should have minimal birefringence. To balance the two beams, a pellicle optical flat (Oriel, Stamford, CT, Model 3740) was placed in one of the beams and the intensity was varied by varying the angle, therefore natural reflectance. We held the beam polarization to vertical and rotated the optical flat in the horizontal plane made by the incident and reflected beams. An even poorer extinction was seen with these substrates due to their being subject to acoustic vibrations. Even with a plastic sheet minimizing the circulation of air in the interferometer, the output fringe was seen to vibrate due to fluttering of the thin optics. A third method of beam splitting and intensity balancing was tried using two half-inch-thick uncoated optical flats. One flat was used as a beam splitter and the other was used as the balancing element, identical to the procedure used for the pellicle optics, but again, no improvement was seen.

The final criteria of intensity uniformity is the most difficult to evaluate, since no information is given on uniformity of reflectivity across the reflecting pieces of optics. Note, that any nonequal reflectance of one mirror versus the other, or the presence of a scatter point in a substrate which only one of the beams must pass, will cause

nonequal intensities at that particular point in the wavefront. We did several spot tests of the extinction at various places on the beam splitter and mirrors, but no significant improvement was seen.

Conclusion

Taking into account the extremely difficult conditions needed to achieve a very low extinction, perhaps a ratio of $2x10^{-5}$ should be looked upon as the best that can be done and, therefore state-of-the-art extinction for destructive interference from a double beam interferometer. The probability of achieving the extinction ratio of 10^{-12} seems low from our experience.

References

1. Borman, S. A. Anal. Chem. 1982, 54, 327A-332A.
2. Harris, J. M.; Dovichi, N. J. Anal. Chem. 1980, 52, 695A-705A.
3. Stone, J. J. Opt. Soc. Am. 1972, 62, 327-33.
4. Stone, J. Appl. Opt. 1973, 12, 1828-30.
5. Patel, C. K. N.; Tam, A. C. Appl. Phys. Lett. 1979, 34, 467-70.
6. Tam, A. C.; Patel, C. K. N. Appl. Opt. 1979, 18, 3348-58.
7. Harris, T. D. Anal. Chem. 1982, 54, 741A-50A.

8. Dovichi, N. J.; Harris, J. M. Anal. Chem. 1980, 52, 2338-42.

9. Cremers, D. A.; Keller, R. A. Appl. Opt. 1982, 21, 1654-62.

10. Michelson, A. A. Amer. J. Sci. 1881, 22, 120-9.

11. Michelson, A. A. Philos. Mag. 1882, 13, 236-43.

12. Born, M.; Wolf, E. "Principles of Optics"; Pergamon Press: New York, 1959; Chapter 7.

13. Connors, C.; Jacobs, S. F. Appl. Opt. 1983, 22, 1794.

14. "Handbook of Chemistry and Physics", 55th ed.; Weast, R. C., ed.; CRC Press: Cleveland, Ohio, 1974; p. D-150.

15. Yeung, E. S.; Steenhoek, L. E.; Woodruff, S. D.; Kuo, J. C. Anal. Chem. 1980, 52, 1399-1402.

PART II. NEW DETECTION METHODS

QUANTITATIVE ION CHROMATOGRAPHY WITH AN ABSORBANCE DETECTOR WITHOUT STANDARDS

Introduction

Ion chromatography has made substantial advances in the last few years (1-3), partly because of the development of new detection methods. Much interest has been centered around nonsuppressed ion chromatography because of the smaller void volumes possible and the greater simplicity in the system. Even though the conductimetric detector works quite well there, several optical methods, including indirect photometric (4), indirect refractive index (RI) (5), and direct photometric (6) methods, have been suggested to improve the overall detectability and to allow the use of more nearly standard liquid chromatographic instrumentation. An interesting question is whether there exists a sensitive absolute method for quantitation in ion chromatography, so that the concentration of ions can be determined as they elute from the column without prior identification and therefore without using standards.

Recently (7), it has been demonstrated that analytes can be quantified without identification in liquid chromatography (LC) by using the refractive index detector, and the method has been applied in gel-permeation chromatography (8). The concept can be extended to the

absorbance detector in LC, and is particularly applicable to ion chromatography.

Theory

In the simplest case of a chromatographic peak registered by an absorbance detector in LC, the response, ΔA, is related to the molar absorptivities of the eluent, ε_1, and the solute, ε_x, by Beer's Law. If m_x and m_1 are the number of moles of the analyte (solute) and the eluent, respectively, in the detection cell of volume, V, (liters) and unit pathlength (1 cm), then the observed absorbance is A as determined by

$$A = \varepsilon_x m_x/V + \varepsilon_1 m_1/V \qquad \ldots (1)$$

For most forms of LC, it is more convenient to work with concentrations in the volume fraction, V_x and $(1-V_x)$, for the solute and the eluent, respectively. If the molar volumes of the solute and the eluent are v_x and v_1, then

$$A = \varepsilon_x V_x/v_x + \varepsilon_1(1-V_x)/v_1 \qquad \ldots (2)$$

where the substitution $m_i = V_i V/v_i$ has been made for each component. When the detection cell contains only the eluent, $A = \varepsilon_1/v_1$ because V_x is zero. In LC, normally a differential absorbance detector is used so that a response, ΔA, is measured with respect to this "baseline".

$$\Delta A = V_x(\varepsilon_x/v_x - \varepsilon_1/v_1) \qquad \ldots (3)$$

The only assumption invoked in Eq. 3 is that of an ideal

solution between the eluent and the solute, but such an assumption is needed in all LC work anyway, in order to relate the concentration observed at the detector to that of the injected sample, which is often present in an unpredictable matrix. Equation 3 has exactly the same form as Eq. 8 in Ref. 7, and allows the application of the quantitative scheme described in Ref. 7 to the absorbance detector in LC. A subtle point is that unlike the refractive index detector, which gives a nonlinear response with respect to concentration, no assumption of low concentration is needed in deriving Eq. 3, to the limit of the working range of Beer's Law.

Very briefly, one can consider Eq. 3 as having two unknowns, V_x and f_x, where f_x is defined to be ε_x/v_x. If one injects the same sample into the LC system using two eluents with different molar absorptivities, ε_1 and ε_2, two different peak areas will be obtained for each separated peak. There are then available two equations of the form in Eq. 3 to solve for the two unknowns, provided that ε_x is the same in both eluents. The concentration as well as the volume-weighted molar absorptivity of the analyte can be thus determined without analyte identification and without the use of standards. If the two eluents can be eluted using each other as the chromatographic mobile phase, one can follow the procedure in Ref. 7 and use Eq. 16 (7) to

calculate the concentration of the analyte without knowing even the molar absorptivities of the two eluents, and without calibrating the response of the detector.

In ion chromatography, some modifications must be made to Eqs. 2 and 3. In general, the major component of the eluent is always non-absorbing (e.g., water). Equation 1 should then refer only to the eluent ions, 1, and the solute ions, x. The principles of electroneutrality and equivalence of exchange imply that the total number of equivalents of the eluting ion and the solute ion remain fixed, because the number of co-ions in the eluent is constant. It is thus more convenient to think in terms of concentrations in normality. The normality of the solute ion with charge, n_x, and the eluting ion with charge, n_1, at the detector are then N_x and (N_1-N_x), respectively, because the normality of the solution is a constant. The concentration of the eluting ion at the eluent reservior is in fact, N_1. Equation 1 can then be rewritten as:

$$A = \varepsilon_x N_x/n_x + \varepsilon_1(N_1-N_x)/n_1 \qquad \ldots (4)$$

Again, because only a differential response, ΔA, is measured Eq. 4 becomes

$$\Delta A = N_x(\varepsilon_x/n_x - \varepsilon_1/n_1) \qquad \ldots (5)$$

If the same sample is then studied with a different eluting ion, 2, such that ε_2/n_2 is quite different from ε_1/n_1, one obtains two independent equations of the form of Eq. 5. The

fact that the major component in each case is identical (e.g., water) guarantees that ε_x is identical in the two eluents. So, one can solve for the two unknowns, N_x and ε_x/n_x.

The use of Eq. 5 requires that the molar absorptivities and the charge numbers of the two eluting ions are known. Sometimes, it is inconvenient to determine ε and n because more than one form of a eluting ion may be present simultaneously, e.g., the various dissociated forms of a polybasic weak acid. These eluents can naturally be used if the equilibrium is controlled by, e.g., the solution pH. If each eluting ion elutes conveniently when the other is used as the eluent, the procedure leading up to Eq. 16 in Ref. 7 can be used to determine the concentration of the solute ion without knowing the physical properties of the eluting ions. If the eluting ions do not conveniently elute in each other, one can arbitrarily choose two additional ions, 3 and 4, to accomplish the same goal. The complete procedure is to first obtain peak areas, S, for the analyte ions in each of the two eluents. Because peak areas take into account all ions that pass through the detector, they are not affected by changes in retention time. Redefining $\varepsilon_i/n_i \equiv F_i$ in Eq. 5, one obtains

$$S_1K_1 = C_x(F_x - F_1) \quad \ldots (6)$$

$$S_2K_2 = C_x(F_x - F_2) \quad \ldots (7)$$

where K_i is a constant characteristic of the particular eluent, including the scale expansion used at the detector, the eluent flow rate, and the integration interval for the area. This K_i then allows the use of arbitrary units for the areas S, and gives the concentration, C_x, at injection rather than at the detector. As long as the same set of chromatographic conditions is used throughout for a given eluent, K_i is a true constant. For the peak areas obtained for ions 3 and 4 in the same two eluents

$$S_3K_1 = C_3(F_3 - F_1) \quad \ldots (8)$$

$$S_4K_2 = C_3(F_3 - F_2) \quad \ldots (9)$$

$$S_5K_1 = C_4(F_4 - F_1) \quad \ldots (10)$$

$$S_6K_2 = C_4(F_4 - F_2) \quad \ldots (11)$$

It is more convenient, but not necessary, to use the same concentration, C, for these two ions, so that $C = C_3 = C_4$. Equations 8 through 11 then give

$$K_2/K_1 = (S_3 - S_5)/(S_4 - S_6) \quad \ldots (12)$$

Now, Eqs. 8 and 9 give

$$(F_2-F_1)/K_1 = [(S_3 - (K_2/K_1)S_4]/C. \quad \ldots (13)$$

Similarly, Eqs. 6 and 7 give

$$(F_2-F_1)/K_1 = [(S_1 - (K_2/K_1)S_2]/C_x \quad \ldots (14)$$

Combining Eqs. 12 through 14, the final result is

$$C_x = C\{S_1-S_2[(S_3-S_5)/(S_4-S_6)]/S_3-$$
$$S_4[(S_3-S5)/(S_4-S_6)]\} \quad \ldots (15)$$

Equation 15 implies that quantitative determination is

possible without knowing any of the absorption properties of the eluents, the analyte ion, or the two "calibrating" ions. The only requirements are that the two absorptivity functions, F_3 and F_4, are quite different, so that (S_3-S_5) and (S_4-S_6) can both be determined with good precision, and that the two functions F_1 and F_2 are quite different (but not necessarily different from F_3 or F_4), so that the subtractions in the numerator and in the denominator of Eq. 15 can retain significance. It is also noted that S_3 through S_6 need only be determined once for a given set of eluting ions 1 and 2.

Once C_x is known, one can calculate the absorptivity of the analyte ion if the absorptivities of the eluting ions are known, following the procedure in Ref. 7. However, in ion chromatography, this is not convenient since the exact distribution of ionic forms of the eluting ion may not be well determined. One can obtain the same information if instead the absorptivities of the "calibrating" ions 3 and 4 are known. From Eqs. 9 and 11:

$$K_2 = C(F_3 - F_4)/(S_4 - S_6) \qquad \ldots (16)$$

From Eqs. 7 and 9:

$$F_x - S_2K_2/C_x = F_3 - S_4K_2/C \qquad \ldots (17)$$

Combining Eqs. 16 and 17:

$$F_x = [(S_2C/C_x - S_4)/(S_4-S_6)](F_3 - F_4) + F_3 \qquad \ldots (18)$$

Experimental

All reagents and eluents used are reagent-grade materials without further purification. Water is deionized and purified by a commercial system (Millipore, Bedford, MA, Milli-Q System). The chromatographic system used was conventional, and consisting of a reciprocating pump (Milton Roy, Riviera Beach, FL, Model 196-0066), a 25-cm x 4.6-mm 15-μm ion chromatographic column (Vydac, Hesperia, CA, 302-IC-4.6), a 25-cm x 4.6-mm 10-μm C_{18} column (Alltech, Deerfield, IL), a 20-μL sample loop at a conventional injection valve (Rheodyne, Berkeley, CA, Model 7010), and a commercial absorbance detector (Rainin, Woburn, MA, Model 153-00) operated at 254 nm. The reference cell was used in the static mode filled with the eluent being used. Flow rates between 0.79 and 1.36 mL/min were used.

The output of the ultraviolet (UV) detector (1 mV full scale) was connected to a digital voltmeter (Keithley, Cleveland, OH, Model 160B), the analog output of which was in turn connected to a computer (Digital Equipment, Maynard, MA, Model PDP 11/10 with LPS-11 laboratory interface). The computer took readings typically every 0.05 s, and averages each set of 10 before storing the information. Typically about 100 of these averaged data points defined an analyte peak. The area is determined by summation of the adjusted values above a chosen baseline for each peak to account for

a slight linear drift in the detector, and the values were used directly as S_1 defined earlier. All areas were determined using multiple injections (three or more). The linearities of the detector and of the attenuation settings were measured by injections of successively diluted samples covering the ranges used in this work.

Absorbances of samples were measured with a conventional spectrophotometer (Shimadzu, Columbia, MD, UV-240).

Results and Discussion

An important condition for deriving Eq. 15 is that the detector response, even though it need not be calibrated, must be linear with respect to concentration. It has already been pointed out (9) that although commercial detectors in general behave properly at low absorbance levels, nonlinearity of response appears even at moderate concentrations. In the particular detector used in this study, stray light and amplifier bias current could affect linearity when the absorbing eluent was used. Therefore, the detector response was measured under chromatographic conditions by injecting five samples spanning a concentration range of a factor of 16 to cover all the scale expansions used in these experiments. The result is a straight line passing through the origin with a slope of

1.001 and a correlation coefficient of 0.9997 when the area, S_i, was plotted against the concentration, each normalized to the highest value. If the peak heights were used instead, the two highest concentrations fell off the straight line. This is expected due to band broadening from saturation in the chromatographic column. Equation 15 can thus be used with confidence. It should be noted that a unit slope is not a necessity in this scheme, because only the value K_2/K_1 is used.

The validity of Eq. 3, was checked by following a procedure similar to that described earlier (7). The two eluents used were cyclohexane and a 0.015 M solution of benzene in cyclohexane. A reversed-phase C_{18} column was used. This provided eluent absorbances of 0.0 and 1.1, respectively, in the 1-cm detector. Ideally, one wants the absorbances of the two eluents to be as different as possible to assure good sensitivity. In practice, highly absorbing eluents block out too much light in the optical path, and stray light plus amplifier bias current become dominant backgrounds. Increasing the intensity of the light source or the amplification of the photoelectric detector is not of much help, because when the absorbance changes from 1 to 10, the fraction of light transmitted changes by a factor of 10^9. By then, other effects such as thermal lensing (10) will become significant. The absorbing eluent is thus

chosen to have an absorbance of about unity. Samples of "unknowns" are prepared by well-defined dilutions of the absorbing eluent in the range 10-100%. On applying Eq. 16 (7), the "unknown" concentrations are predicted with an accuracy of ±2%, within the uncertainties of the area measurements. This indicates that Eq. 3 holds even at these high volume fractions, in contrast to the case of the refractive index detector.

The verification of Eq. 3 under conditions for reversed-phase chromography does not imply that this scheme is useful for LC in general. An examination of Eq. 3 reveals that the detector response (ΔA) must have a numerically significant difference in the two eluents. For eluents having absorbances of 0.0 and 1.0, respectively, and a detector capable of measuring an absorbance change of 2×10^{-4} in either eluent, one essentially has a dynamic reserve of 5×10^{3}. So, the volume fraction of the analyte must be at least 2×10^{-4} at the detector. Considering an additional dilution factor for the concentration at injection, this is a relatively high concentration for the analyte. It is noteworthy that the situation is identical regardless of the molar absorptivity of the analyte. For comparison, the refractive index detector typically can detect changes in the order of 10^{-7} RI units. For two eluents with RI differences of 0.1 units, this is a dynamic

reserve of 1 x 10^6. The useful concentration range is then extended by a factor of 200. So, we have the curious result that the RI detector offers lower detection limits than the absorbance detector for most LC applications of this quantitation scheme.

In ion chromatography, the situation is quite different. The major component in each eluent, e.g., water, plays no part in determining the response given by Eqs. 4 and 5. Each equivalent of an analyte replaces one equivalent of the eluting ion. The dynamic reserve for absorption measurements discussed above then refers to the fraction of eluting ion that is exchanged by the analyte ion. Because the former is usually already at a low concentration, the detection limit for the analyte can be quite impressive. In contrast, if an RI detector is used for ion chromatography (5), the difference in RI dictated by the two eluting ions is small because of the presence of the major component. The detectability based on RI will be, therefore, no better in ion chromatography than in any other form of LC.

To test the applicability of this scheme in ion chromatography, a 10^{-3} M solution of potassium hydrogen phthalate and a 10^{-3} M solution of potassium citrate were chosen as the two eluents. The former has a measured absorbance of 1.31 and the latter has a measured absorbance

of 1.6×10^{-4} at 254 nm in a 1 cm cell. Both are adjusted to pH 5.4 with potassium hydroxide to avoid changes in ε_x for the analytes caused by pH effects. At this pH, the eluents were each a mixture of different ionic species, the ratios of which were not measured. Because the absorptivities of the citrates are essentially zero, their exact distribution is not critical. For the phthalates, since the isobestic point is not used, the pH is chosen in a self-buffered region to minimize changes as the analyte ion elutes. Care must be taken if a buffering agent is used, because there is chance that charge balance at the detector involves the buffer ion as well and Eq. 4 will not be strictly valid. If the ion-exchange mechanism involves a constant ratio of eluting versus buffer ions, Eq. 4 can be used, but with a loss in sensitivity. The analyte ions chosen were IO_3^-, NO_2^-, Br^-, NO_3^-, and $SO_4^=$, to provide a range of absorptivities and charge, and to have reasonably well-behaved elution on the column used. Figure 1 shows the chromatograms of two test mixtures eluted by phthalate ions, and Figure 2 shows the chromatograms of the same mixtures eluted by citrate ions. The chromatograms show good separation for the ions, so that area determination should be reliable. Flow rates of 0.79 mL/min for the phthalate ions and 0.94 mL/min for the citrate ions were used. This, plus the difference in elution strengths of the ions,

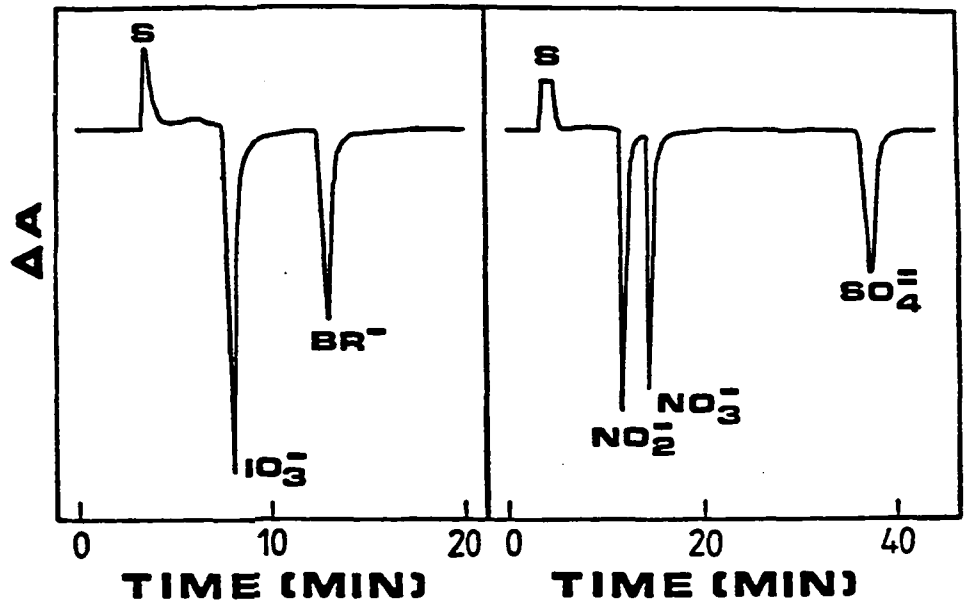

Figure 1. Absorption chromatograms of two mixtures of ions using phthalate ions as the eluent. S is the solvent peak. Concentrations are as listed in Table 1. Full scale corresponds to 0.08 absorbance units

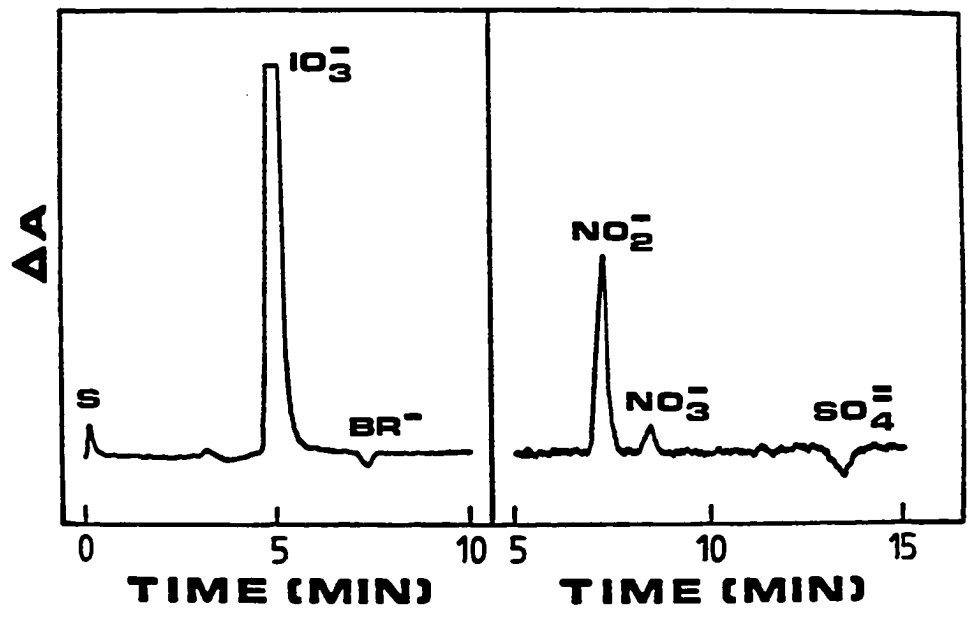

Figure 2. Absorption chromatograms of two mixures of ions using citrate ions as the eluent. S is the solvent peak. The concentrations are as in Figure 1. Full scale corresponds to 0.005 and 0.0025 absorbance units for the left and right displays, respectively

resulted in different elution times for the analyte. As mentioned earlier, the flow rates are included in the constants, K_1 and K_2, and should not affect quantitation. Because one can safely assume a fixed elution order for ions in the two eluents, the more involvd "consistency" test discussed earlier (7) can be omitted. In the left display of Figure 2, the scale is chosen to display the small peak due to bromide. The iodate peak is actually within the range of digitization of the computer, and peaks at about 4x full scale.

The results of the experiments are summarized in Table 1. The areas measured (three or more injections) by the computer for the two mixtures in each eluent are tabulated as S_1 and S_2. The integration interval in each eluting ion is different to allow optimized data collection over each chromatographic peak. The A/D interface used produced a value of 2048 for full-scale deflection, and all areas were normalized to the 0.005 scale on the detector. The actual absorbance corresponding to full-scale deflection, however, was not determined. For each of the ions, the normal concentration was calculated from the weight of material used in preparing the samples, and these are listed together with the known absorptivities of each ion. The concentrations of the last three ions were also checked by independent analysis. There are many combination of ions

Table 1. Quantitation of analyte ions

Ion	IO_3^-	Br^-	NO_2^-	NO_3^-	$SO_4^=$
S_1[a] (x10^3)	-393.8 ± 6.10	-228.2 ± 3.41	-349.1 ± 4.05	362.9 ± 4.03	-422.6 ± 1.74
S_2[b] (x10^3)	256.2 ± 2.45	-2.130 ± .0904	15.07 ± .492	1.860 ± .235	-4.310 ± .544
True C_x[c]	1.14	0.62	0.97	1.01	1.20
True ε_x/n_x[d]	150	0	12	4.0	0
Calc. C_x[e,f]	---	---	0.95 ± .02	0.99 ± .02	1.15 ± .02
Calc. ε_x/n_x[e,g]	---	---	12.7 ± .4	3.5 ± .2	-0.1 ± .3
Calc. C_x[f,h]	1.07 ± .29	0.64 ± .01	---	---	1.18 ± .02
Calc. ε_x/n_x[g,h]	143. ± 38.	1.0 ± .2	---	---	0.8 ± .4

[a] Integration interval - 2 S; 2048 = F.S. on 0.005 scale; eluent - phthalate.

[b] Integration interval - 0.5 S; 2048 = F.S. on 0.005 scale; eluent - citrate.

[c] $(x10^{-3}N)$.

[d] Values obtained from Ref. 11.

[e] IO_3^- and Br^- used as the "calibrating" ions.

[f] Eq. 15.

[g] Eq. 18.

[h] NO_2^- and NO_3^- used as the "calibrating" ions.

that can be chosen as the "calibrating" ions 3 and 4. The results for two of these combinations are tabulated. The error estimates in Table 1 are determined from the propagation of errors in the measured areas. To account for the fact that C_3 is not equal to C_4, the areas are first normalized to a concentration of C = 1 x 10^{-3} N for the two ions before applying Eqs. 15 and 18.

One has to be careful in applying Eqs. 15 and 18 to be sure that the subtractions result in significant numbers. This can be illustrated using iodate as ion 3 and bromide as ion 4. Using the areas in Table 1, one obtains for the normalized areas (S_3-S_5) = (-345400 + 368100) = 22700, and (S_4-S_6) = (224700 + 3440) = 228100. Considering that the areas are reliable to 2-3% for those in the 100,000's and to 10-15% for those in the 1,000's, (S_4-S_6) is reliable to 2-3%, but (S_3-S_5) is only reliable to 30-50%. The factor K_2/K_1, the order of 0.1, is then only determined to an accuracy of 30-50%. However, because for the other three ions, S_2 is quite small compared to S_1, the numerator in Eq. 15 essentially maintains the 2-3% reliability dictated by S_1 alone. For the denominator in Eq. 15, one has the choice of using that form or the equivalent form of $(S_5-S_6(K_2/K_1))$. If the former is used, a slightly larger uncertainty will result because of the relative magnitudes of S_3 and S_4, but the uncertainty is still only 3-4%. If the latter is used,

one can improve the reliability again to 2-3%. It is therefore not surprising that the concentrations calculated for the "unknowns" in Table 1 are quite good, i.e., with errors less than 4%. If instead nitrite is used as ion 3 and nitrate is used as ion 4, K_2/K_1 has a value of -0.043 with an uncertainty of factor of 10. For predictions of the concentrations of bromide and sulfate, this is not a problem because S_2 is substantially smaller than S_1. For the case of iodate, the net uncertainty is of the order of 20%. This explains the results in Table 1, where bromide and sulfate are predicted with good accuracy and iodate is in error by 6%. This confirms the discussion earlier that for the best accuracy, F_3 and F_4 should be as different as possible. The present results would have been even better if an ion with higher absorptivity than iodate had been used as ion 3 and any nonabsorbing ion as ion 4. A subtle point is that the reliability of the predictions is independent of the absorptivity of the analyte ion as long as it is within the linear range of the detector used.

To determine the absorptivities of the ions, one can either use Eq. 16 to determine K_2 or use $K_1 = C(F_3-F_4)/(S_3-S_5)$. A slightly different set of indices will be present in Eq. 18 in the latter case. From the concentration-weighted areas, one finds that (S_4-S_6) has much smaller uncertainties than (S_3-S_5) regardless of which pair of ions in Table 1 are

chosen as ions 3 and 4. So, the former choice should be used. The predicted normal absorptivities are quite good when iodate and bromide are used for "calibration". The prediction for sulfate of -0.1 is close enough to zero to make the negative sign insignificant. The predicted absorptivities are also good when nitrite and nitrate are used, but not as good as the other values. This is because there is more uncertainty in the literature values (11) for the absorptivities of these two ions. In general, one wants to have F_3 and F_4 as different as possible to improve the reliability of Eq. 18.

There is sufficient information to determine the absorptivities of the eluting ions as well. From Eq. (9), $F_2 = F_3 - S_4K_2/C_3$. Using iodate as ion 3 and bromide as ion 4, one finds that $F_2 = 2.3$. The uncertainty is about 100% because of the subtraction of two numbers of the order of 150. This is consistent with the independent measurement of $F_2 = 0.2$ for the citrate solution used. From Eq. 8, $F_1 = F_3 - S_3K_1/C_3$. One finds $F_1 = 2440$ compared to the value of 1370 measured independently. The literature value (11) of 1700 is for the monohydrogenated ion only, and cannot be used for comparison. The large discrepancy is due to the uncertainly in determining K_1, producing an uncertainty of 50%. Obviously, to obtain better values for the absorptivities of the eluting ions, one needs a larger

difference in F_3 and F_4, so that extrapolation will not be over such an extended range.

To check the dynamic range of the method as well as some of the operating parameters, a series of chromatograms was obtained with nitrate as the analyte ion at five concentration (at injection) of 8×10^{-3} N to 5×10^{-4} N, in steps of two. The injection loop used has a calibrated volume of 0.477 times that of our 20-L loop, The integration interval was chosen to be 4 times shorter than that used earlier, and the flow rate was a factor of 1.72 higher. So, the areas obtained for this series of samples are first multiplied by factors to normalize them to the same sample size, the same integration interval, and the same flow rate. Equation 15 was then used to predict the concentrations. The result was a average error of 3.9% with the mean, i.e., the least-square straight line using all five samples, deviating only 0.7% from the "true" value. This is particularly significant because these experiments were performed one week after the initial series that produced the calibration. So, as long as these operating parameters can be related to those used earlier, the "calibration" remains good. Judging from the noise on the baseline on the most sensitive scales used for each eluent, it should be possible to measure an area for nitrate at a concentration of 1.25×10^{-5} N and 5-μL injection. This

corresponds to 4 ng of ions injected, and is comparable to detection limits reported for indirect absorbance detection (4). For analytical scale LC, injections of even 200 μL will not degrade the chromatographic resolution substantially, so that a concentration of 3×10^{-7} N should be adequate. This is consistent with the dynamic range of absorption detectors of 5×10^{3} and an eluting ion concentration of 1×10^{-3} N. It is possible to use another eluting ion, or phthalate ions at another absorption wavelength, so that F_1 is larger by as much as a factor of 120. The detection limit can then be improved accordingly, because the concentration of the eluting ion can then be decreased and yet maintain a background absorbance of about 1.0. For micro scale LC, the absolute detection limit can be improved because the elution volume of a given peak can be substantially smaller. An ion with a larger F_1 must be used to accommodate the typically shorter absorption pathlengths in order to benefit from this fact. A detectability of 10 pg should be feasible. The detectability, just like the reliability of Eq. 15, is independent of the absorptivity of the analyte.

The procedure above allows the determination of the number of equivalents of an analyte. Retention times in ion chromatography are related to charge numbers. Specifically, if the logarithm of the adjusted retention time is plotted

against the logarithm of the concentration of the eluting ion, the slopes are in the ratios of the charge numbers of the ions (12). Therefore, the elution of the same 5 ions was studied at other concentrations of the eluting ions. It was found that sulfate has a slope twice that of the other 4 ions. This implies that n_x can be independently determined for each without analyte identification. Molar concentrations can thus be derived from Table 1, as well as molar absorptivities.

Finally, the relationship between this scheme and some others needs to be discussed. The use of ion-interaction chromatography in conjunction with a UV detector (13) is an inselective method for quantifing ions. However, the absorbance of ion-interaction reagents can be affected differently by different analyte ions, so that only approximate concentrations can be determined without standards. Indirect photometric methods for ion chromatography (4) have truly constant sensitivity for all nonabsorbing ions, but then one must assume or know that the analyte ion is in fact nonabsorbing. Indirect refractive index detection can easily be adapted to this scheme for quantitation, but, as pointed out above, it is somewhat less sensitive than the current scheme even if properly optimized. It is naturally possible, for example, to pass the chromatographic effluent into a strong-base anion-

exchange resin in the hydroxide form and then relate the amount of hydroxide ions created to the normality of the analyte ion, but the procedure is tedious and suffers from possible degradation of the separatory power. In comparison with the RI scheme reported earlier (7,8), the current absorbance scheme using Eq. 3 gives exactly the same results for most forms of LC, but with poorer sensitivity. When adapted to ion chromatography based on Eq. 5, the sensitivity is impressive, but then the response is no longer truly universal, i.e., only analytes in ionic forms will be determined.

Conclusion

The quantitation scheme developed for LC uses the absorbance detector in a mode that does not require identification of the analyte and does not require knowing any of its physical properties. The scheme is verified using anion chromatography, but the extension to cations is straightforward.

References

1. Small, H. In "Trace Analysis"; Lawrence, J. F., Ed., Academic Press: New York, 1982; Vol. I, p. 267.
2. Fritz, J. S.; Grerde, D. T.; Pohlandt, C. "Ion Chromatography"; Huthig: New York, 1982.

3. Small, H. Anal. Chem. 1983, 55, 235A-42A.

4. Small, H.; Miller, T. E. Anal. Chem. 1982, 54, 462-9.

5. Haddad, P. R.; Heckenberg, A. L. J. Chromatogr. 1982, 252, 177-84.

6. Reeve, R. N. J. Chromatogr. 1979, 177, 393-7.

7. Synovec, R. E.; Yeung, E. S. Anal. Chem. 1983, 55, 1599-1603.

8. Synovec, R. E.; Yeung, E. S. J. Chromatogr. 1984, 283, 183-5.

9. McDowell, L. M.; Barber, W. E.; Carr, P. W. Anal. Chem. 1981, 53, 1373-6.

10. Swofford, R. L. In "Lasers and Chemical Analysis"; Heiftje, G. M.; Travis, J. C.; Lytle, F. E., Eds.; Humana Press: Clifton, NJ, 1980; p. 143.

11. "UV Atlas of Organic Compounds"; Plenum: New York, 1971; Vol. V.

12. Gjerde, D. T.; Schmuckler, G.; Fritz, J. S. J. Chromatogr. 1980, 187, 35-45.

13. Barber, W. E.; Carr, P. W. J. Chromatogr. 1983, 260, 89-96.

QUANTITATIVE ION CHROMATOGRAPHY WITHOUT STANDARDS BY CONDUCTIVITY DETECTION

Introduction

Ion chromatography has developed into a very useful analytical technique in the past few years (1-3). Research in the development of low capacity columns and in detection methods has reached the point where suppression of the eluent conductance is no longer necessary (4-6). Methods of ion detection other than by conductivity have been developed and some give slightly better overall detectabilities. However, the conductivity detector has some advantages and remains the most common detector for use in ion chromatography.

Recently, we showed that absorbance due to samples of ions eluted successively be a strongly absorbing ion and by a weakly absorbing ion can be used to determine the concentrations and the molar absorptivities of the sample ions (7). In what follows, we shall show that the conductivity detector can also be used as a detector in this quantitative scheme. Although the conductivity detector may show a slightly poorer overall detectability, it allows better characterization of most inorganic ions. This is because most inorganic ions do not absorb in the visible or near-UV spectral regions (8,9). So, even though our scheme

allows the determination of the molar absorptivities (7), these are not very useful for characterizing the ions. With the use of the conductivity detector, this problem is solved due to the wide range of equivalent ionic conductances that inorganic ions display.

Theory

The conductance of a solution of ions is related to their equivalent ionic conductances and their concentrations. The conductance of a solution of ions consisting of one anion and one cation, as is the case for a self-buffered eluent, is

$$G = C(\lambda_+^0 + \lambda_-^0)/1000K \quad \ldots (1)$$

C is the concentration (normality) of the ions, G is the conductance (mhos), and K is the cell constant (cm^{-1}). λ_+^0 and λ_-^0 are the limiting equivalent conductances of the cation and anion, respectively. These closely approximate the actual equivalent conductances of the ions in dilute solutions (10^{-3} to 10^{-5} N), such as those used in single column ion chromatography (2). This equation can be used to predict the background conductance of a chromatographic eluent.

The conductance of a chromatographic effluent consisting of sample ions being eluted by an eluent can similarly be described. For example, in the case of a

single analyte (anion) being eluted through a column, the conductance is predicted by

$$G_s = [C_E\lambda_E^+ + (C_E - C_s)\lambda_E^- + C_s\lambda_s^-]/1000K \quad \ldots (2)$$

where λ_E^+ and λ_E^- are the equivalent conductances of the eluent (cation and anion, respectively) and λ_s^- is the equivalent conductance of the sample anion. The eluent and sample concentrations (normalities) are C_E and C_s. In Eq. 2, the principles of electroneutrality and equivalence of exchange require that the total number of equivalents of cations equals the total number of anions. Regardless of the particular cation that was associated with the analyte anion at injection, only the eluent cation is relevant at the chromatographic peak.

A differential conductivity detector does not measure the actual conductance, but rather a change in the conductance of the effluent stream. To derive an equation for the change in conductance, ΔG, we need only subtract the conductance of the eluent above, as predicted by Eq. 1, from the conductance of the eluent and sample ions, as predicted by Eq. 2. Thus we obtain

$$\Delta G = C_s(\lambda_s^- - \lambda_E^-)/1000K. \quad \ldots (3)$$

Eq. 3 has exactly the same form as Eq. 5 in Ref. 7 and as Eq. 8 in Ref. 10. One can easily see that this detector can be used for the quantitative method described in detail in Ref. 7 and 10.

Briefly, the method consists of measuring the chromatographic peak areas of the analyte ion in each of two eluents that have anions with different equivalent conductances. Two equations of the form in Eq. 3 can be thus obtained to solve for the two unknowns, C_s and λ_s^-. The concentration is then determined without analyte identification and without standards. To avoid being influenced by uncertainties in the values of λ_E^- for the two eluents or in the instrumental calibration factors, one can instead measure the peak areas, S, for the analyte ion in each of the two eluents, such that

$$S_1K_1 = C_x(F_x - F_1) \quad \ldots (4)$$

and

$$S_2K_2 = C_x(F_x - F_2) \quad \ldots (5)$$

where we redefine $\lambda_i \equiv F_i$, with the subscripts x designating the unknown and 1 and 2 the eluents, and use a proportionality constant, K_i. There are two methods of calibrating the response from the detector, so that one does not need to determine K_i or any physical properties of the eluent F_i in order to calculate the concentration of analyte ions injected onto the column. The only requirement is that the experimental conditions, e.g., temperature, remain fixed for each of the eluents. The simplest method of calibration is to measure the peak area of each of the eluting ions eluted from the column using the other as the eluent at

known concentrations, C_1 and C_2. This will allow us to obtain areas S_a and S_b, such that

$$S_aK_1 = C_2(F_2 - F_1) \quad \ldots (6)$$

$$S_bK_2 = C_1(F_1 - F_2). \quad \ldots (7)$$

From Eqs. 4 through 7, using the derivation detailed in Ref. 10, we arrive at an expression for C_x

$$C_x = \left(\frac{S_1C_2}{S_a} + \frac{S_2C_1}{S_b}\right) \quad \ldots (8)$$

One can also calculate the equivalent conductance of the analyte ion, if one knows the equivalent conductances of the eluent ions. The equation for F_x can be derived from Eqs. 15 and 17 of Ref. 10. With these substitutions, the equation becomes

$$F_x = \frac{F_2\left(\frac{S_1S_bC_2}{S_2S_aC_1}\right) + F_1}{\left(\frac{S_1S_bC_2}{S_2S_aC_1}\right) + 1} \quad \ldots (9)$$

The second method of calibrating the detector's response is to use two "calibrating" ions, 3 and 4. Thus, one can calibrate even in the case where one eluent ions does not elute off the column using the other eluent ion within a reasonable amount of time. The two calibrating ions allow us to obtain four additional relationships

$$S_3K_1 = C_3(F_3 - F_1) \quad \ldots (10)$$

$$S_4K_2 = C_3(F_3 - F_2) \quad \ldots (11)$$

$$S_5K_1 = C_4(F_4 - F_1) \quad \ldots (12)$$

$$S_6K_2 = C_4(F_4 - F_2). \quad \ldots (13)$$

These plus Eqs. 4 and 5 can be manipulated, as shown in Ref. 7, to arrive at the following expression for C_x:

$$C_x = \left[\frac{S_1 - S_2\left(\frac{S_3/C_3 - S_5/C_4}{S_4/C_3 - S_6/C_4}\right)}{S_3 - S_4\left(\frac{S_3/C_3 - S_5/C_4}{S_4/C_3 - S_6/C_4}\right)}\right] C_3 \quad \ldots (14)$$

As before (7), we may solve for the equivalent conductance of the analyte ion if we know the equivalent conductance of the calibrating ions 3 and 4, using the following equation

$$F_x = \left[\frac{S_2/C_x - S_4/C_3}{S_4/C_3 - S_6/C_4}\right] (F_3 - F_4) + F_3 \quad \ldots (15)$$

Experimental

All reagents and eluents used are reagent grade materials without further purification. Water is deionized and purified by a commercial system (Millipore, Bedford, MA, Milli-Q System). The chromatographic system used is conventional, and consists of a syringe pump (ISCO, Lincoln, NE, Model 314), a 25-cm x 4.6-mm 15-μm ion chromatography column (Vydac, Hesperia, CA, 302 IC 4.6), a 20-μL sample loop on a conventional injection valve (Rheodyne, Berkeley, CA, Model 7010), and a commercial differential conductivity detector (Wescan Instruments, Santa Clara, CA, Model 214). The flow rates used were between 1.33 and 1.66 mL/min.

The output of the conductivity detector (1 V full scale) is connected to a computer (Digital Equipment, Maynard, MA, Model PDP 11/10 with LPS-11 Laboratory interface). The computer takes readings every 0.05 s and averages every set of 10 before storing the information. Typically, about 100 of these averaged data points define an analyte peak. The area is determined by summation of the adjusted values above a chosen baseline for each peak to account for a slight linear drift in the detector, and the values are used directly as S_i defined earlier. All areas are determined using averages of multiple injections (three or more).

Results and Discussion

The conductivity detector is known from previous work to be linear within the range of concentrations used for ion chromatography. So, there was no need for special calibration.

When choosing eluents for this scheme it is important to choose two ions which have very different equivalent conductances and which are well-behaved and strong eluents. The different equivalent conductances are needed in order to obtain distinct chromatograms, so that the responses S_1 and S_2 will be very different. Otherwise, we cannot obtain a significant solution to Eqs. 4 and 5. We chose the ions

thiosulfate, $S_2O_3^{=}$, and benzoate. In order to maximize sensitivity, we did not use buffer ions, which would have possibly participated in the ion exchange mechanisms.

There can be a problem when using a weak acid as an eluent. If there is some of the unionized acid, HA, in the eluent, then when the sample displaces some of the anion form, A^-, some of the HA will dissociate to replace the A^-. This has an effect of enhancing the detection sensitivity slightly (2), but causes the response at the detector not to behave according to Eq. 3. For the same reason, suppressed ion chromatography (4) cannot be used with this scheme, due to the signal enhancement by the suppressor column. Furthermore, the conductance of the eluting ion does not participate in the detector response in suppressed ion chromatography, and two independent equations cannot be obtained to solve for the two unknowns.

It is generally assumed that in selecting an eluent with a high conductance per ion, one would have to work with a background conductance too high for the conductivity detector to maintain its sensitivity. This is however not a problem due to the large range in the offset adjustment and the possibility of a dual-cell arrangement in modern detectors. The noise level does increase with the background conductance because of temperature and flow fluctuations. However, with syringe pumps and proper

thermal insulation, we found that good signal-to-noise ratios can still be obtained in eluents with conductivities in the 100 mho range. Moreover, one can find ions with high equivalent conductances that are also strong eluents, so that these can be used at lower concentrations to provide a low background. In our case, the high conductance eluent ($S_2O_3^=$) was used at a concentration of 6 x 10^{-4} M at pH 6.1, while the low conductance eluent (benzoate) was used a 5 x 10^{-3} M at pH 6.1. It is interesting to calculate the background conductance of each eluent from Eq. 1. Using the equivalent conductance of 50.1 mho-cm^2/equivalent for the counterion, Na^+, and a cell constant, K, of 30 cm^{-1}, the $S_2O_3^=$ eluent has a background conductance of 5.4 μmhos, while the benzoate eluent has a background conductance of 14 μmhos. Thus, we have the odd case of the high conductance eluent having the lower background. When choosing the low conductance eluent, a good choice would have been phthalate ions due to its being a stronger eluent. One therefore has a lower background conductance than if benzoate is used. Although one would lose some sensitivity due to phthalate having a slightly higher equivalent conductance than benzoate, one would still gain in detectability from the lower noise level. To avoid changes in equilibrium, one should work at a pH of 7.4 to make sure most of the phthalate is doubly ionized. This pH range is however not

suitable for the particular column used here. Also, phthalate does not elute conveniently when $S_2O_3^=$ is used, and cannot be used to test Eq. 8. An additional point is that Na^+ has a lower equivalent conductance than K^+. Therefore, Na^+ is the better choice of counterion in terms of reducing background conductance.

The sample ions chosen are trichloroacetate and $SO_4^=$, which with the eluting ions of benzoate and $S_2O_3^=$ provide a wide range of equivalent conductances and charges. Using the eluting ions as calibrating ions, that is, eluting the eluent ions in each other, allows one to make use of the simpler calibration procedure, and thus use Eqs. 8 and 9 to calculate C_x and F_x. Using trichloroacetate and $S_2O_3^=$ as two "calibrating" ions allows one to use Eqs. 14 and 15 for the calculations. Two "unknown" solutions were therefore prepared, one with the two eluting ions, and another with the two sample ions. These were eluted successively with the two eluents as shown in Figures 1 and 2. The chromatograms show good separation for the test ions, so that area determination should be reliable. The nitrate ion was not used as a test ion due to a lack of baseline resolution between it and the solvent peak.

The results are shown in Table 1. The areas measured (three or more injections) by the computer for the four sample ions in each eluent are tabulated as S_1 and S_2.

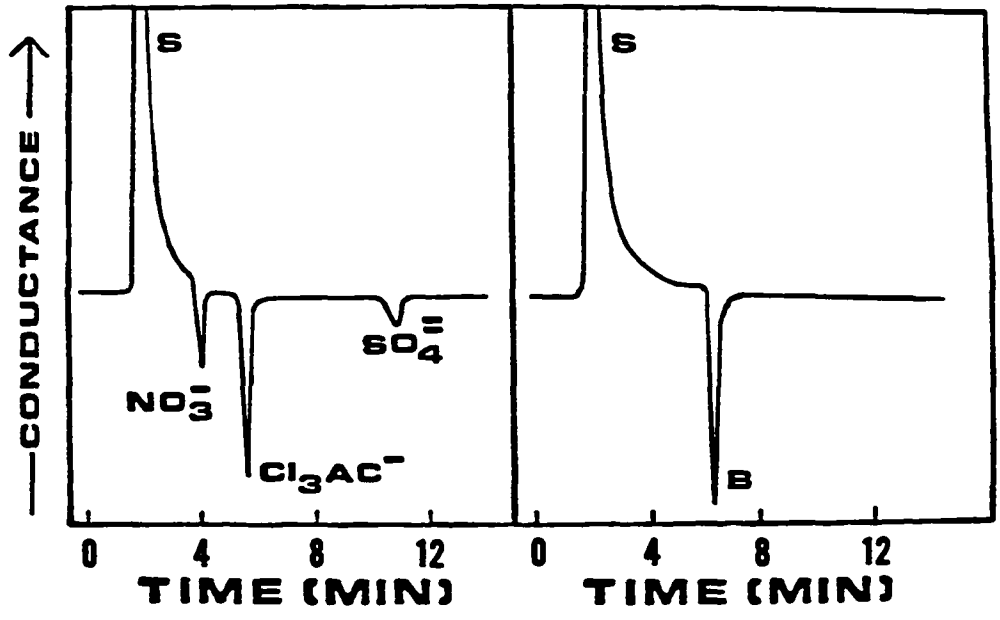

Figure 1. Conductance chromatograms of two mixtures of ions using thiosulfate as the eluent. S, solvent peak; NO_3^-, nitrate; Cl_3AC^-, trichloroacetate; $SO_4^=$, sulfate; B, benzoate. Concentrations are as listed in table 1. Full scale corresponds to 0.5 μmhos

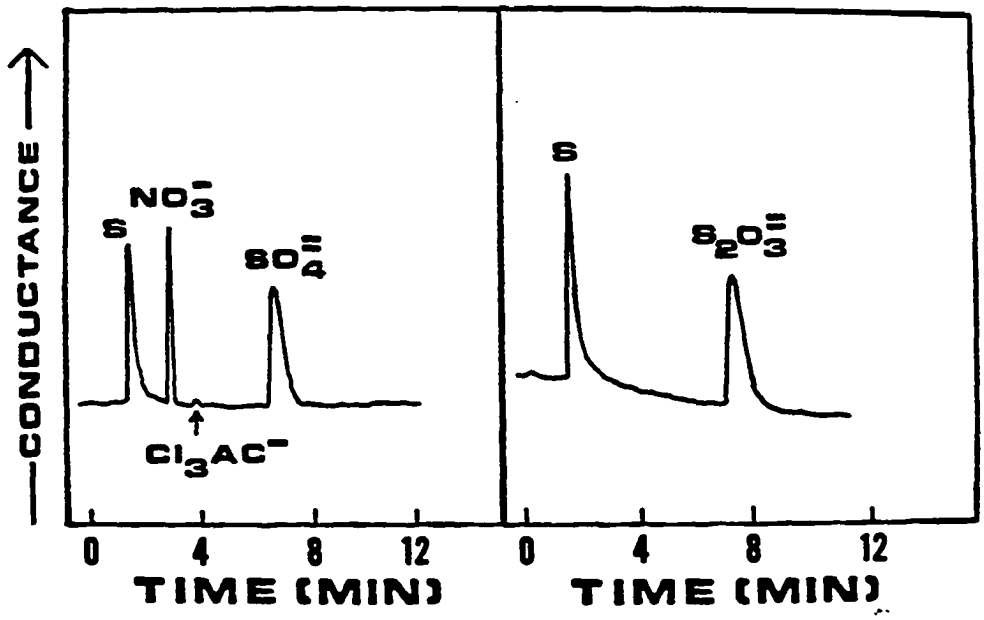

Figure 2. Conductance chromatograms of two mixtures of ions using benzoate as the eluent. Concentrations and labels are as in Figure 1, except $S_2O_3^{=}$, thiosulfate. Full scale corresponds to 0.5 μmhos

There is no difficulty in correlating the chromatographic peaks in the two eluents, since the elution orders are expected to be the same. The integration interval is 0.5 s and our A/D interface produces a value of 2048 for full scale deflection. The actual conductance corresponding to full-scale deflection, however, was not needed in the calculations. For each of the ions, the "true" normal concentration was calculated from the weight of the material used in preparing the samples. These are listed in Table 1 together with the known limiting equivalent conductance of each ion. Equations 8 and 9, or 14 and 15 are then applied directly. It should be noted that one must be careful when applying these equations to be sure that the subtractions result in significant numbers. A detailed discussion of an example dealing with significance is given in Ref. 7. The error estimates in Table 1 are determined from the propagation of errors in the measured areas. Table 1 shows that agreement between the calculated values and the "true" values is good, when either one of the two calibration procedures is used.

An important subtle point with this procedure is that the method has constant sensitivity regardless of the equivalent conductance of the analyte ion. If the ion at moderate concentrations should give a small peak area with one eluent, it will give a large peak area in the other

Table 1. Quantitative data for analyte ions

Ion	Benzoate	$S_2O_3^=$	Trichloroacetate	$SO_4^=$
S_1[a]	0	25,330 ± 686	330 ± 47	18,300 ± 402
S_2[b]	-20,060 ± 124	0	-14,560 ± 163	-3,949 ± 42
True $C_x(x10^{-3}N)$	2.72	4.90	1.98	4.02
True λ_x[c]	32.4	85.0	36.6	80.0
Calc. $C_x(x10^{-3}N)$[d,e]	--	--	2.04 ± .03	4.08 ± .12
Calc. λ_x[d,f]	--	--	34.0 ± .2	78.1 ± .2
Calc. $C_x(x10^{-3}N)$[g,h]	2.64 ± .04	4.85 ± .17	--	--
Calc. λ_x[g,i]	34.9 ± 1.1	86.7 ± .1	--	--

[a]Integration interval - 0.5 S; 2048 = F.S. on 1.0 μ mhos scale; eluent - benzoate; flow rate = 1.66 ml/min.

[b]Integration interval - 0.5 S; 2048 = F.S. on 1.0 μ mhos scale; eluent - $S_2O_3^=$; flow rate = 1.33 ml/min.

[c]Values obtained from Ref. 11.

[d]Benzoate and $S_2O_3^=$ used as the "calibrating" ions.

[e]Eq. 8.

[f]Eq. 9.

[g]Trichloroacetate and $SO_4^=$ used as the "calibrating" ions.

[h]Eq. 14.

[i]Eq. 15.

eluent, due to the large difference in the equivalent conductances of the eluting ions. This implies that the detectability here is as good as, if not better than, standard procedures in nonsuppressed ion chromatography (5), if the two eluting ions are properly chosen. Detectability naturally depends on the efficiency of the column and the retention time of the particular ion. For the benzoate ion in this work, the retention time is 6.3 min. For a typical commercial column for anion chromatography, one has about 6000 theoretical plates. This means that a 20-μL injection of 5×10^{-6} N solution of benzoate ions will have a S/N = 3 at the peak maximum in this detector. The system therefore provides a detectability of 11 ng. Compared to the detectability using a UV absorbance detector (7), this is slightly inferior. However, as discussed above, the large variety of equivalent conductances among ions compared to absorbance provides more information for characterization of the ions.

The procedure above allows for the determination of the number of equivalents of an analyte. One notes that retention times in ion chromatography are related to charge numbers. Specifically, if the logarithm of the adjusted retention time is plotted against the logarithm of the concentration of the eluting ion, the slopes are in the ratios of the charge number of the ions (6). From a study

of the retention times of the four ions as a function of eluent concentration, we found that $SO_4^=$ and $S_2O_3^=$ gave slopes twice that of the other two ions. Thus, we are able to determine the charge on the ions whenever they are considered to be the analyte and can calculate their molar concentrations and molar conductances also.

The method described here can be used with other pairs of eluting ions as well. In general, one wants these to have high eluting powers so that low concentrations of these can be used. The ion exchange columns should have as low a capacity as possible for the same reason. Some possible candidates are the $Fe(CN)_6^{-3}$ and $Fe(CN)_6^{-4}$ anions as the high-conductance eluent and double ionized phthalate ions as the low-conductance eluent, if suitable column are available. For cation chromatography, our scheme should work equally well. There, H^+ and double charged ethylenediammonium ions are good high-conductance eluents, and UO_2^{+2} and larger, doubly charged, organic diammonium ions are good low-conductance eluents. Ion chromatography is somewhat unique in that it is possible to preserve the elution order of a given set of analyte ions even if the eluting ion is changed. So, the chromatographic peaks are correlated and a "consistency test" (10) is not needed in applying our calculations to each analyte peak.

Finally, it is appropriate to ask whether the

conductivity detector, as applied to ion chromatography, can be used for quantitation without standards in some other scheme. The only other possibility is a modification of suppressed ion chromatography (4). In the anion version, the suppressor column converts the eluting anion and an equal equivalent of its conjugate cation to an associated weak acid. The analyte anion passes unmodified with a corresponding equivalent of hydrogen ions. If now one passes the effluent directly into a third column with, e.g., an anion exchanger in the Cl^- form, all the analyte anions will be replaced by Cl^- ions at equal equivalent amounts. The net result is that regardless of the injected anion (or its associated cation), each equivalent will become one equivalent of H^+ ions plus one equivalent of Cl^- ions. The conductivity detector thus shows the same response for any injected anion, provided it is not suppressed in the second column. Quantitation without standards is then achieved. The analogue in suppressed cation chromatography is to use a third column with, e.g., a cation exchanger in the Na^+ form. In some ways, this is analogous to the concept of "replacement" ion chromatography (12). There, column bleeding results in a nonnegligible background, which in turn creates flicker noise in the emission measurement. Using the conductivity detector, however, the background due to column bleeding can be adequately compensated for in a

dual-cell arrangement. This is supported by the results in Table 1, which are obtained in the presence of a substantial background conductance. Naturally, in addition to complexities in regenerating these suppressor and converter columns, band broadening will occur in these schemes because of the added volume, and chromatographic efficiency is degraded. So, the single-column method described above is still preferable.

Conclusion

In summary, we have demonstrated a quantitation method for ion chromatography by using the conductivity detector which does not require identification or knowledge of the physical properties of the analyte ion. The method is shown for the case of anion chromatography, but can also be performed with cation chromatography.

References

1. Small, H. In "Trace Analysis"; Lawrence, J. F. Ed.; Academic Press: New York, 1982; Vol. I, p. 267.
2. Fritz, J. S.; Gjerde, D. T.; Pohlandt, C. "Ion Chromatography"; Huthig: New York, 1982.
3. Small, H. Anal. Chem. 1983, 55, 235A-42A.
4. Small, H.; Stevens, T. S.; Bauman, W. C. Anal Chem. 1975, 47, 1801-09.

5. Gjerde, D. T.; Fritz, J. S.; Schmuckler, G. J. Chromatogr. 1979, 186, 509-19.

6. Gjerde, D. T.; Schmuckler, G.; Fritz, J. S. J. Chromatogr. 1980, 187, 35-45.

7. Wilson, S. A.; Yeung, E. S. Anal. Chim. Acta, 1984, 157, 53-63.

8. Small, H.; MIller, T. E. Anal. Chem. 1982, 54, 462-9.

9. Williams, R. J. Anal. Chem. 1983, 55, 851-4.

10. Synovec, R. E.; Yeung, E. S. Anal. Chem. 1983, 55, 1599-1603.

11. "Lange's Handbook of Chemistry", 11th Ed.; Dean, J. A., Ed.; McGraw-Hill: New York, 1973; p. 6-35.

12. Downey, S. W.; Hieftje, G. M. Anal. Chim. Acta 1983, 153, 1-13.

CONCLUSION

The two parts of this dissertation have described four projects which have lead to improvements in detection techniques and methods. In part I, first a laser-based small-volume flow cell was shown to allow simultaneous detection in LC by monitoring refractive index (ng), absorbance (pg), and fluorescence (sub-pg). Next a laser-based absorbance detector was described which allows for differential measurements by using Michelson interferometry. In part II, a novel detection method allowing quantitative analysis without qualitative was shown to work with the absorbance detector, and then with the conductivity detector for ion chromatography.

ACKNOWLEDGEMENTS

I wish to express my appreciation to Dr. Edward S. Yeung for his guidance and this opportunity.

All of the members of my research group also deserve my thanks for their fellowship and support, especially my officemate, Don Bobbitt and his wife, Susan. My classmates, Bryan, Carmen, Judy, and Russ, were very supportive and will not be forgotten.

For their encouragement and support, I would like to thank my parents, Frances and Carl Wilson, also my brother and sisters: Ken, Rita, Ruby, Carleen, and Juanita.

In the five years I've lived in Ames, I've had the same roommate, Gary Landers. He's a Texan with a heart of gold to whom I wish all the success he deserves.

Finally, a special note of appreciation goes to my friends, the patrons of "Dave's Bike Shop", for all the therapeutic recreation.